Annex A. Motion trajectories of contact points for cylindrical and hemispheric piezorobots

A.1. Contact point trajectories of the cylindrical piezorobot

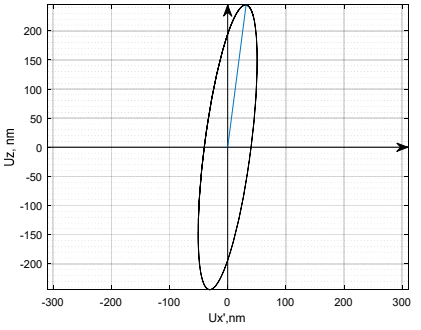

1a) Trajectory of the first contact point (100 V/50 V)

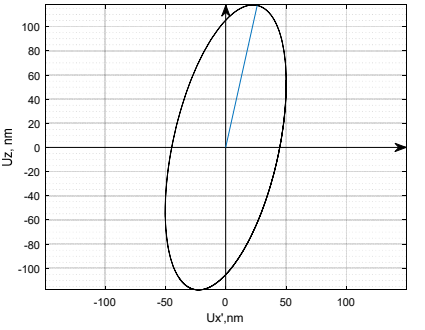

1b) Trajectory of the second contact point (100 V/50 V)

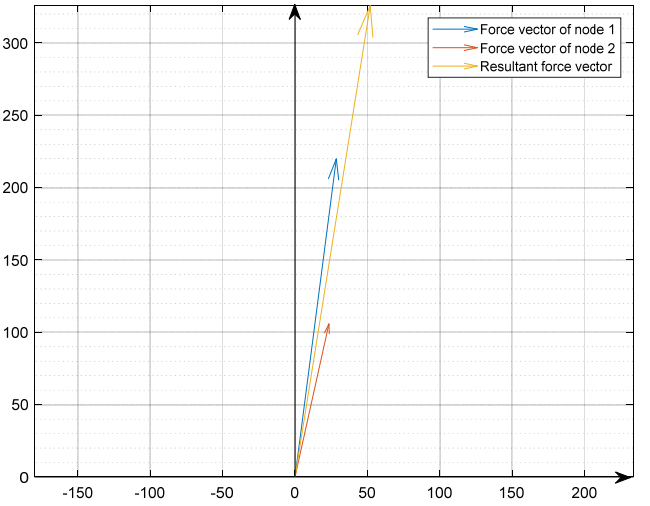

1c) $\varphi = 80.93°, r = 66.61$ nm

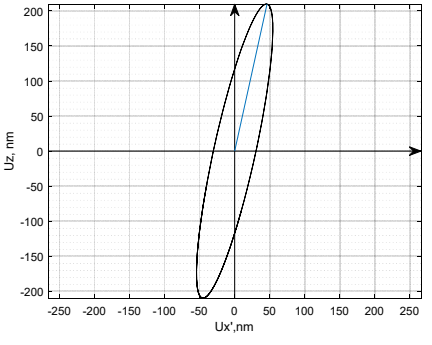

2a) Trajectory of the first contact point (100V/75V)

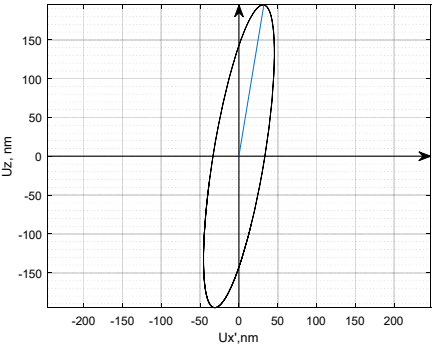

2b) Trajectory of the second contact point (100V/75V)

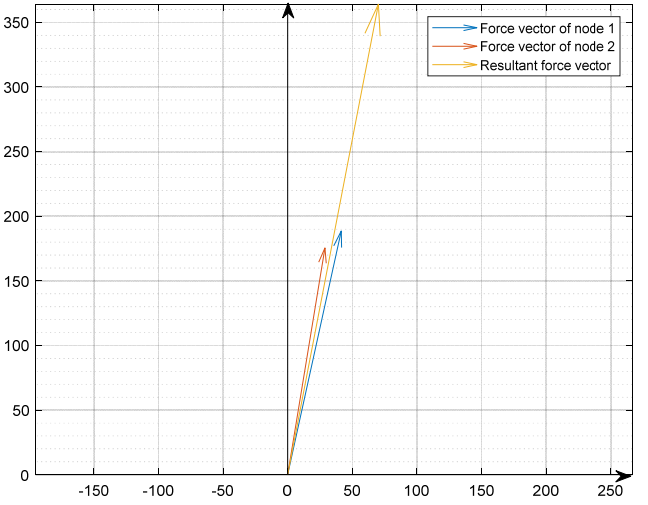

2c) $\varphi = 79.08°$, $r = 412$ nm

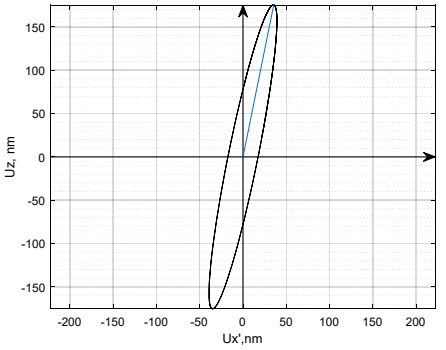

3a) Trajectory of the first contact point (100V/100V)

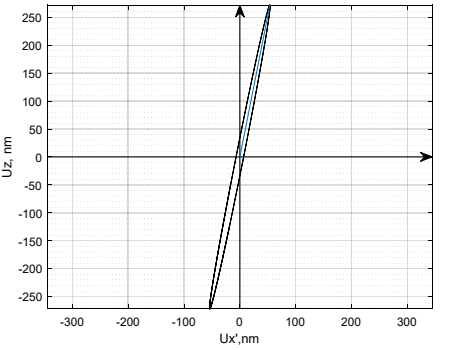

3b) Trajectory of the second contact point (100V/100V)

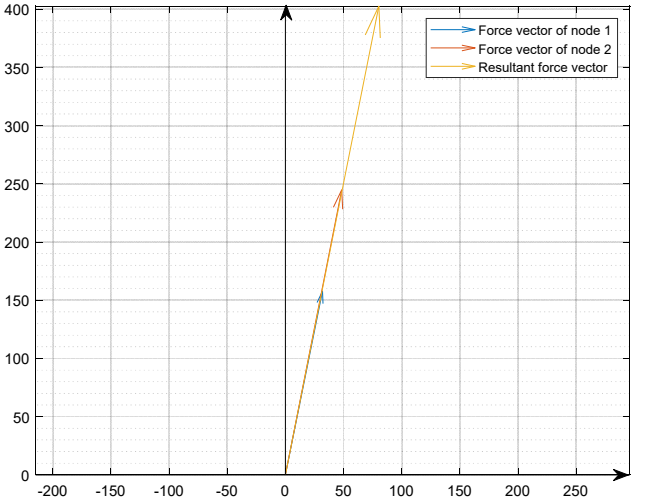

3c) φ =78.72°, r =456.1667nm

Fig. A1. Motion trajectories of contact points of a 10 mm × 12.5 mm × 21 mm cylinder with rectangular electrode scheme

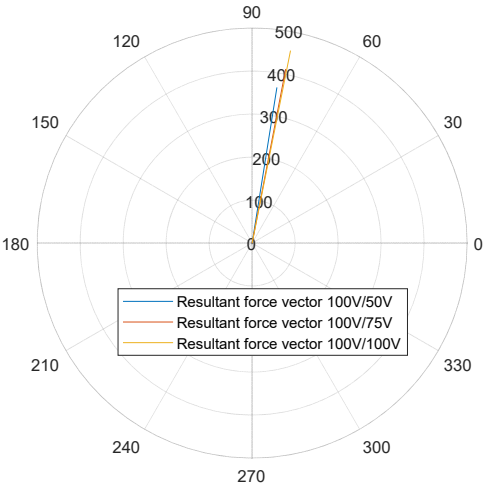

Fig. A2. Resultant force vectors in polar coordinates of contact points of a 10 mm × 12.5 mm × 21 mm cylinder with rectangular electrode scheme

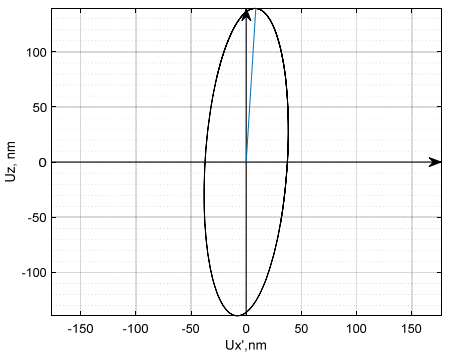

1a) Trajectory of the first contact point (100 V/50 V)

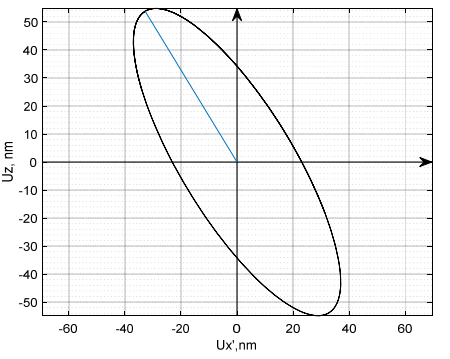

1b) Trajectory of the second contact point (100 V/50 V)

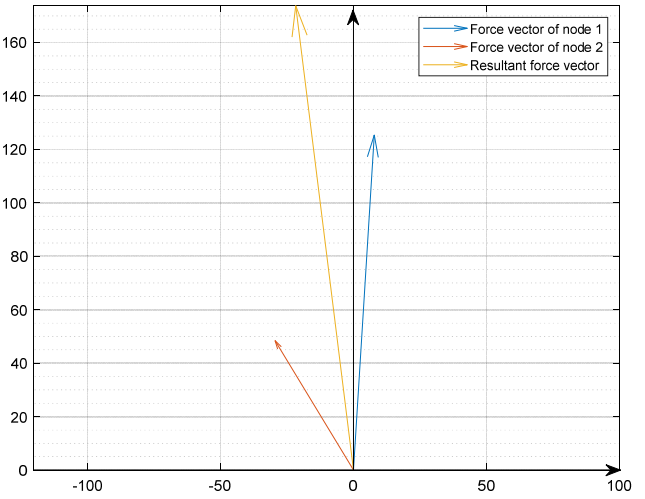

1c) φ =82.8893°, r =194.6221 nm

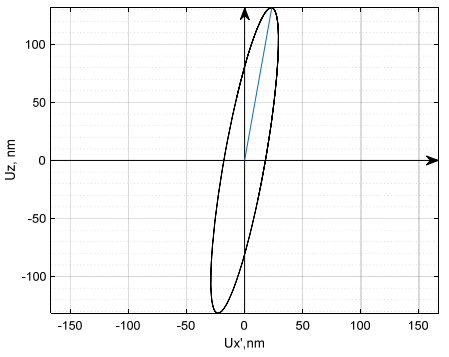

2a) Trajectory of the first contact point (100 V/75 V)

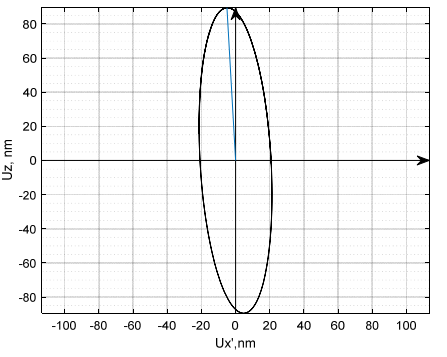

2b) Trajectory of the second contact point (100 V/75 V)

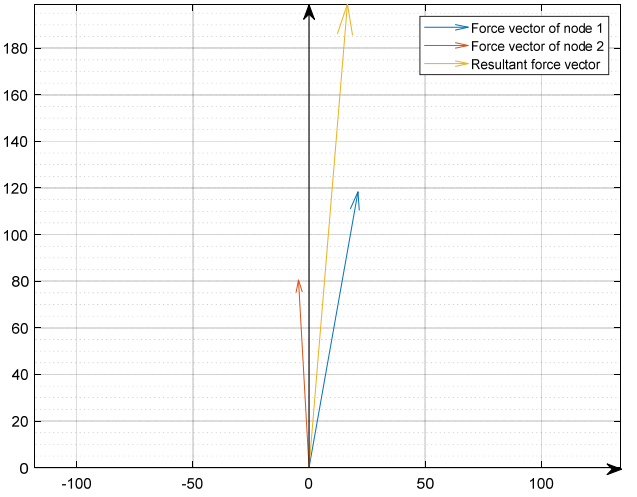

2c) φ =85.2556°, r =221.7510 nm

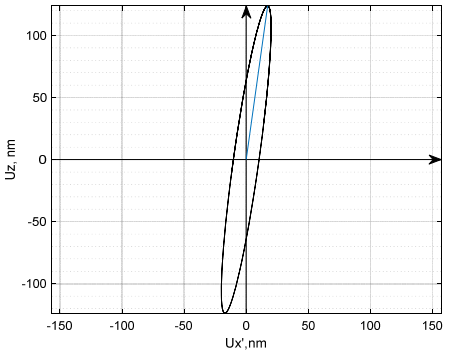

3a) Trajectory of the first contact point (100 V/100 V)

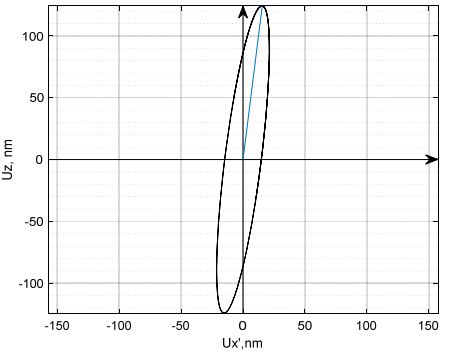

3b) Trajectory of the second contact point (100 V/100 V)

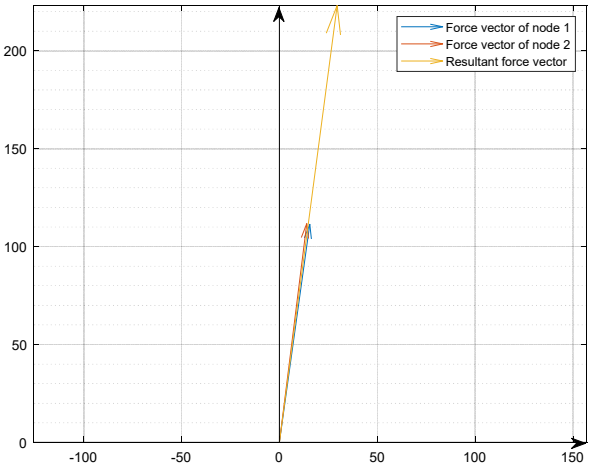

3c) φ =82.4686°, r =250.0585 nm

Fig. A3. Motion trajectories of contact points of a 10 mm × 12.5 mm × 21 mm cylinder with triangular electrode scheme

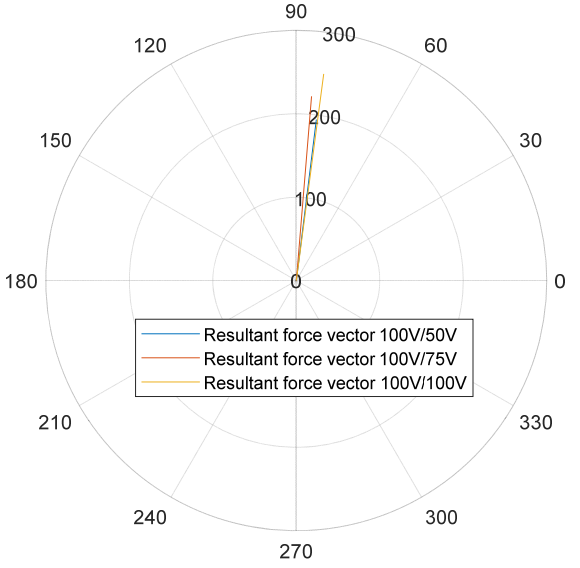

Fig. A4. Resultant force vectors in polar coordinates of contact points of a 10 mm × 12.5 mm × 21 mm cylinder with triangular electrode scheme

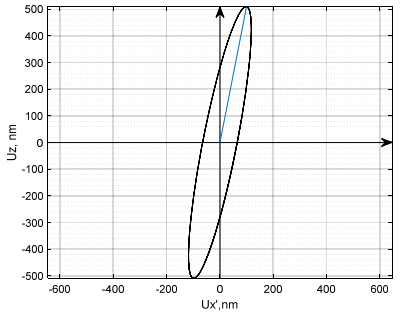

1a) Trajectory of the first contact point (100 V/50 V)

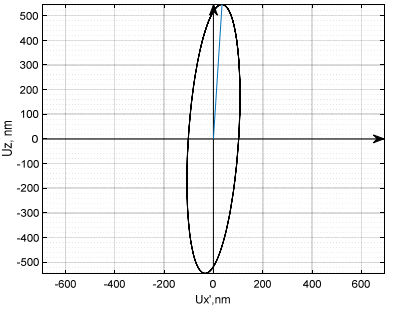

1b) Trajectory of the second contact point (100 V/50 V)

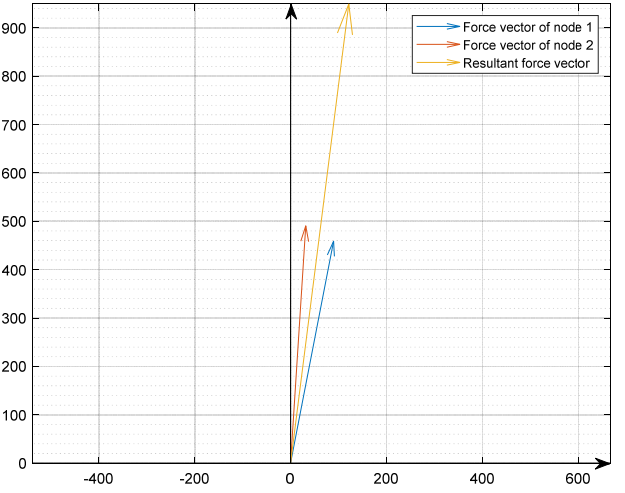

1c) φ =82.7218°, r =1063.3 nm

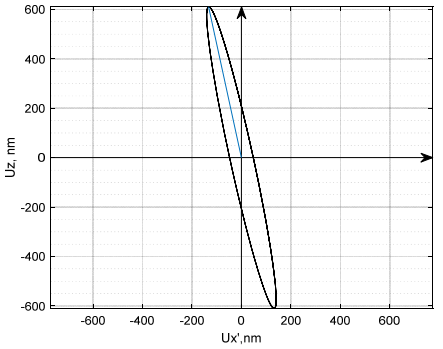

2a) Trajectory of the first contact point (100 V/75 V)

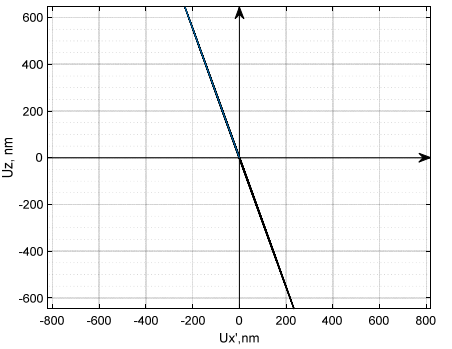

2b) Trajectory of the second contact point (100 V/75 V)

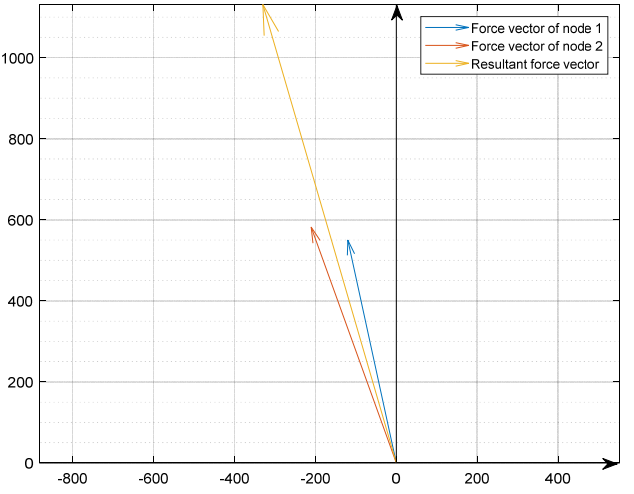

2c) φ =73.7514°, r =1308.8 nm

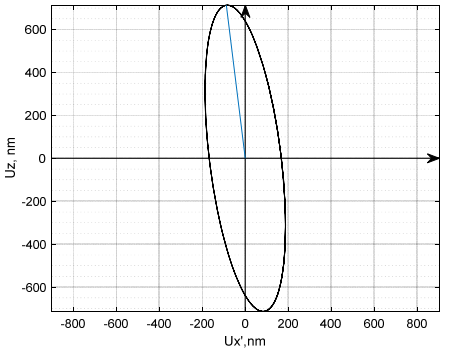

3a) Trajectory of the first contact point (100 V/100 V)

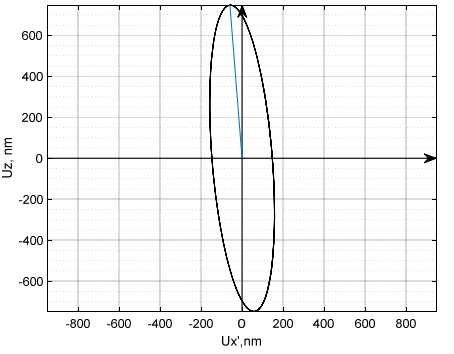

3b) Trajectory of the second contact point (100 V/100 V)

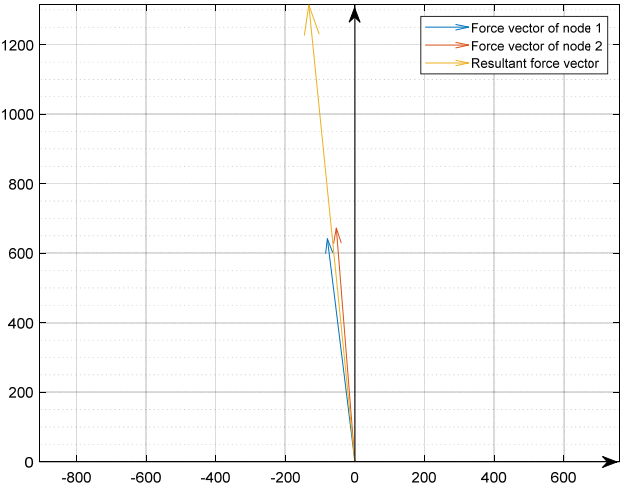

3c) φ =84.2359°, r =1467.8 nm

Fig. A5. Motion trajectories of contact points of a 12 mm × 14.5 mm × 21 mm cylinder with rectangular electrode scheme

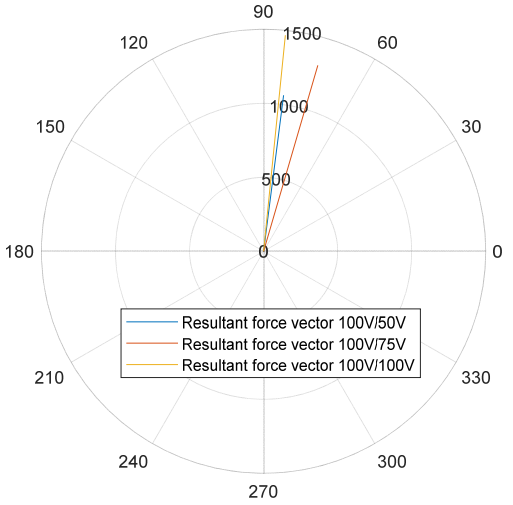

Fig. A6. Resultant force vectors in polar coordinates of contact points of a 12 mm × 14.5 mm × 21 mm cylinder with rectangular electrode scheme

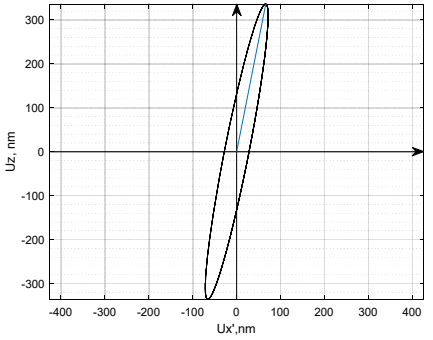

1a) Trajectory of the first contact point (100 V/50 V)

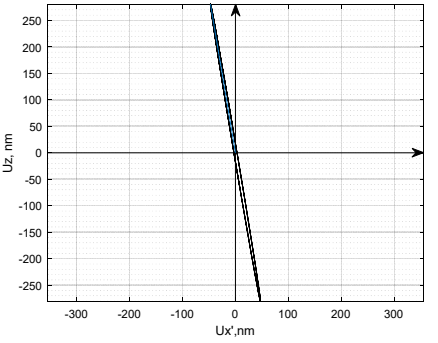

1b) Trajectory of the second contact point (100 V/50 V)

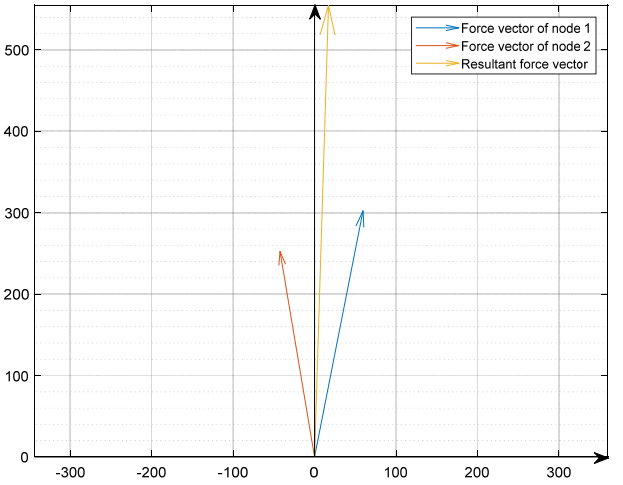

1c) $\varphi = 88.2318°$, $r = 616.8208$ nm

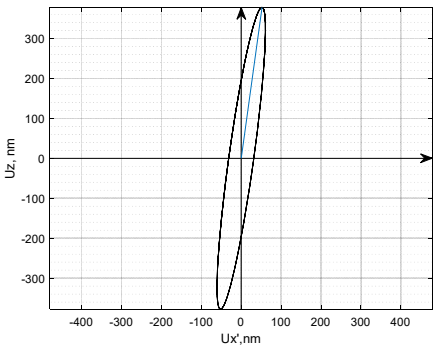

2a) Trajectory of the first contact point (100 V/75 V)

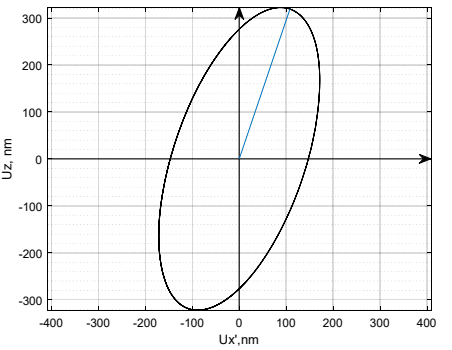

2b) Trajectory of the second contact point (100 V/75 V)

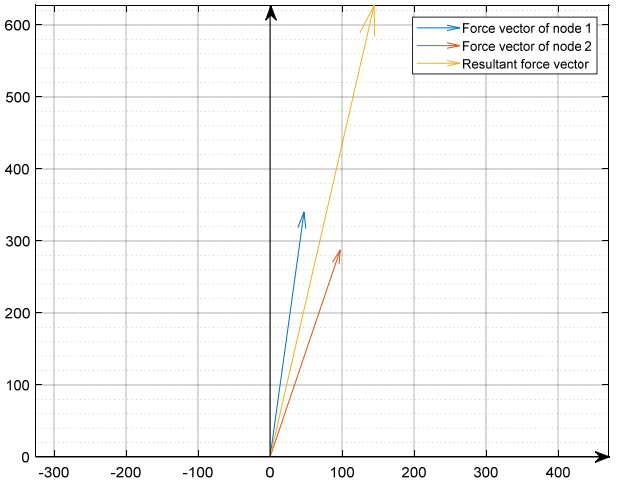

2c) $\varphi = 77.0549°, r = 715.2131$ nm

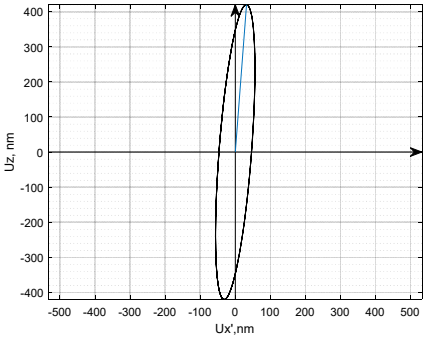

3a) Trajectory of the first contact point (100 V/100 V)

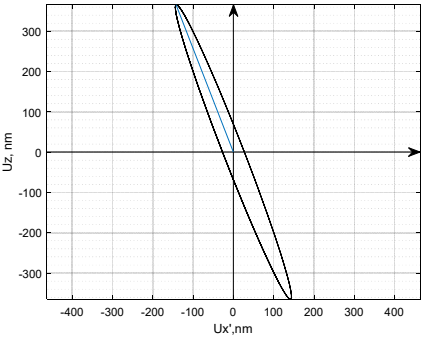

3b) Trajectory of the second contact point (100 V/100 V)

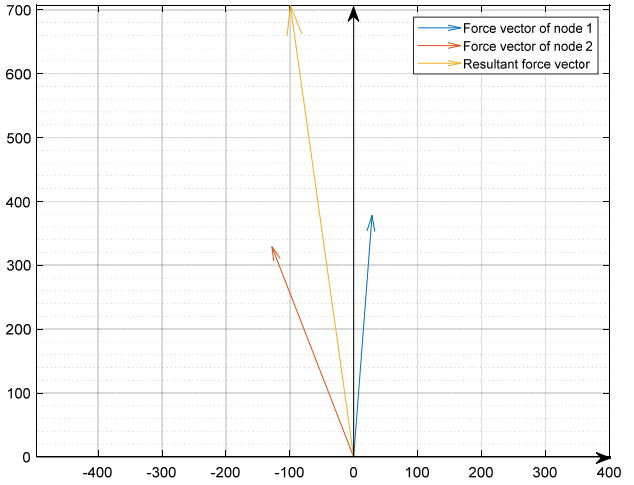

3c) $\varphi = 82.0181°, r = 793.2521$ nm

Fig. A7. Motion trajectories of contact points of a 12 mm × 14.5 mm × 21 mm cylinder with triangular electrode scheme

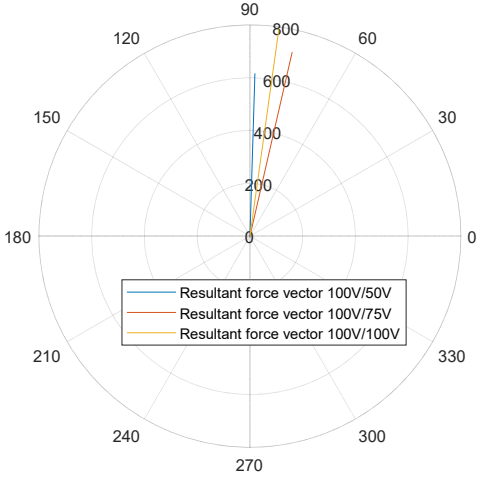

Fig. A8. Resultant force vectors in polar coordinates of contact points of a 12 mm × 14.5 mm × 21 mm cylinder with triangular electrode scheme

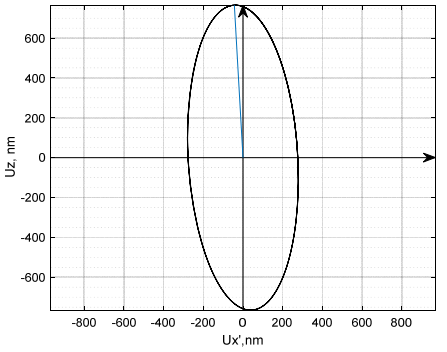

1a) Trajectory of the first contact point (100 V/50 V)

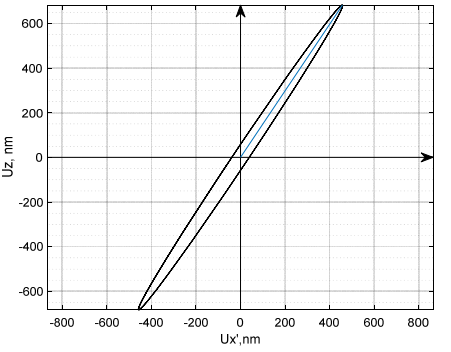

1b) Trajectory of the second contact point (100 V/50 V)

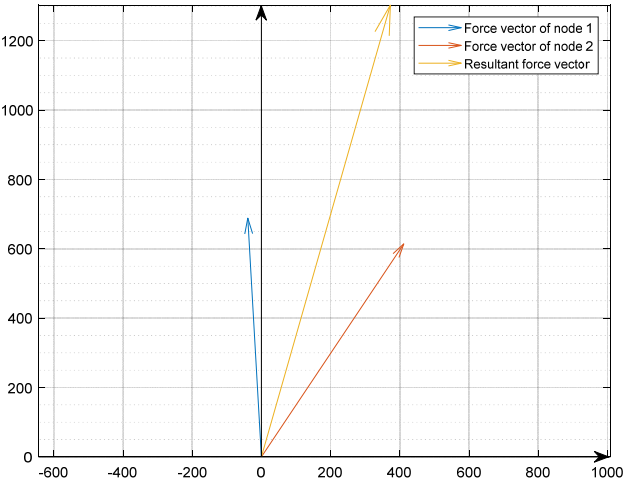

1c) φ =74.0295°, r =1505.4 nm

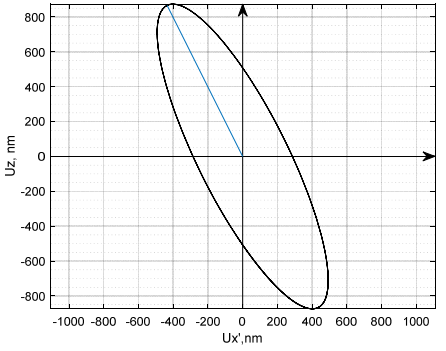

2a) Trajectory of the first contact point (100 V/75 V)

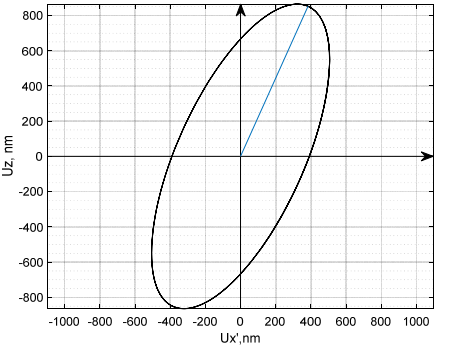

2b) Trajectory of the second contact point (100 V/75 V)

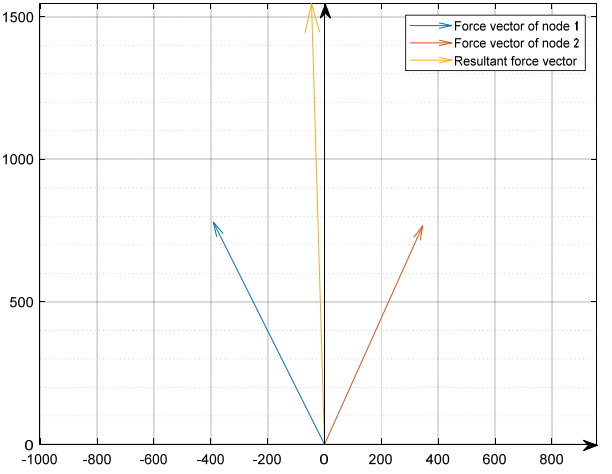

2c) φ =88.3142°, r =1718.8 nm

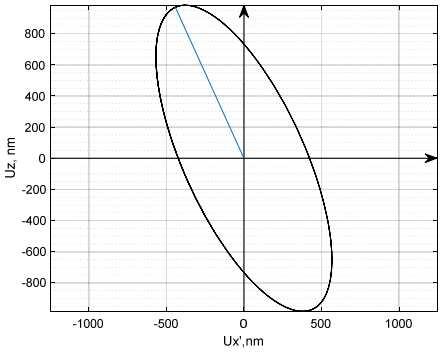

3a) Trajectory of the first contact point (100 V/100ΦV)

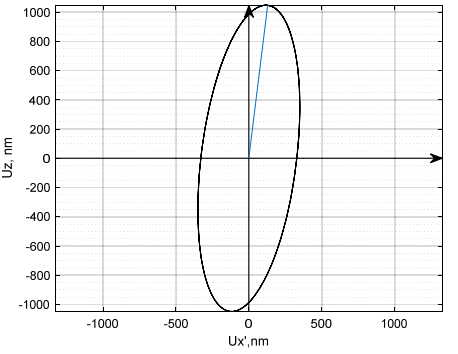

3b) Trajectory of the second contact point (100 V/100 V)

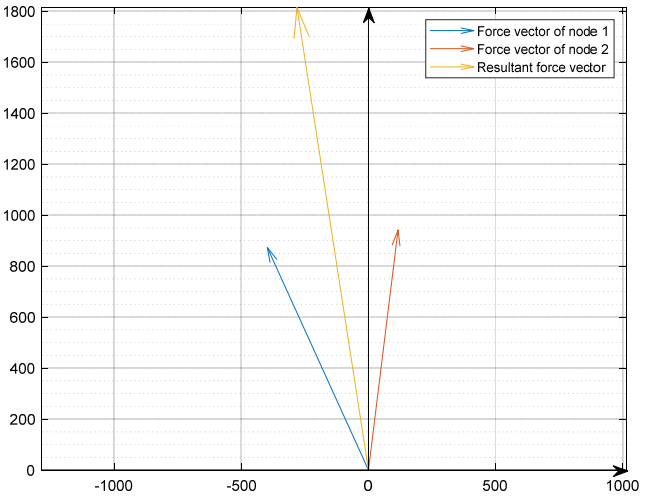

3c) φ =81.1842°, r =2040.7 nm

Fig. A9. Motion trajectories of contact points of a 16 mm × 18.5 mm × 21 mm cylinder with rectangular electrode scheme

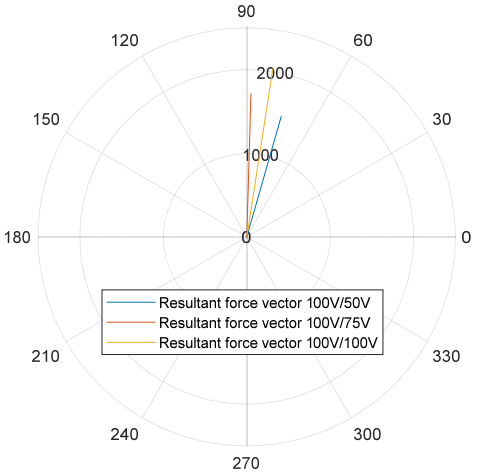

Fig. A10. Resultant force vectors in polar coordinates of contact points of a 16 mm × 18.5 mm × 21 mm cylinder with rectangular electrode scheme

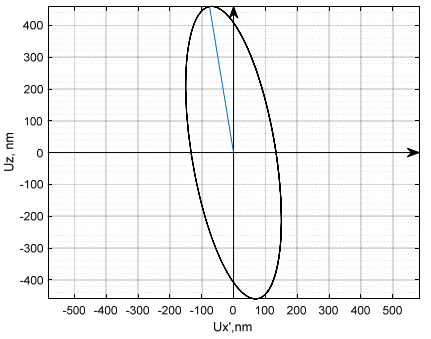

1a) Trajectory of the first contact point (100 V/50 V)

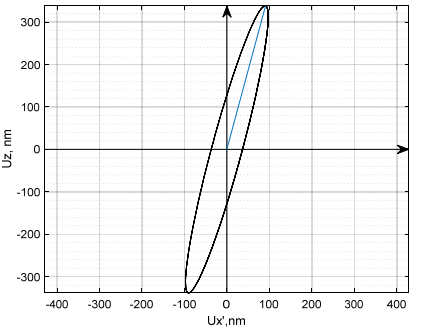

1b) Trajectory of the second contact point (100 V/50 V)

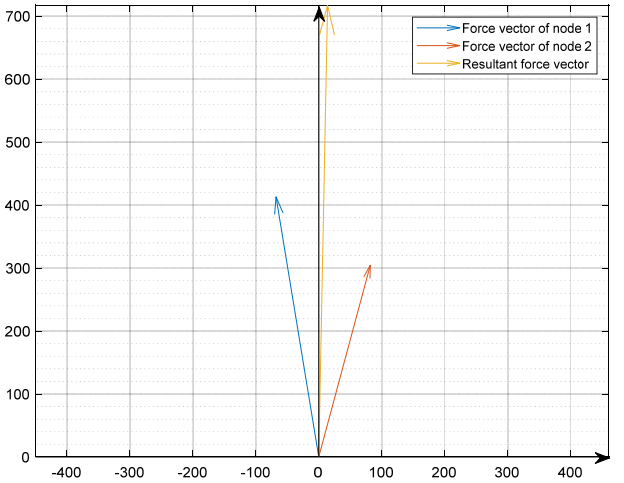

1c) φ =88.8766°, r =797.3268 nm

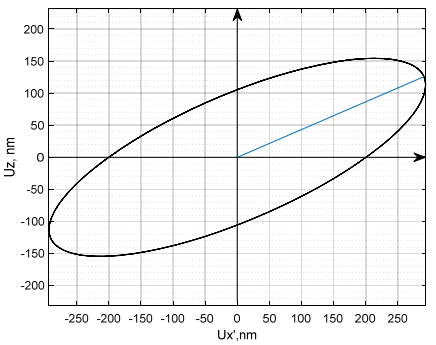

2a) Trajectory of the first contact point (100 V/75 V)

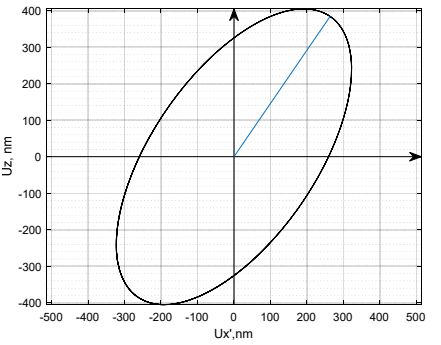

2b) Trajectory of the second contact point (100 V/75 V)

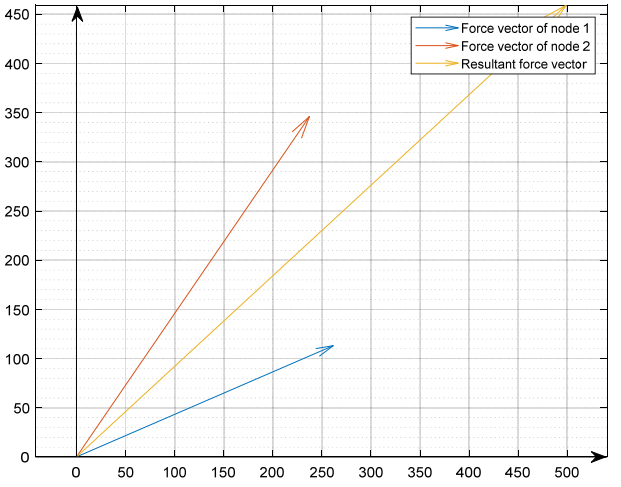

2c) φ =42.6306°, r =753.3368 nm

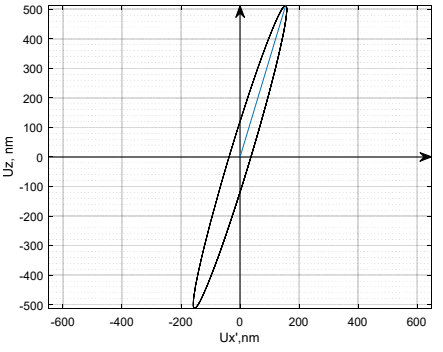

3a) Trajectory of the first contact point (100 V/100 V)

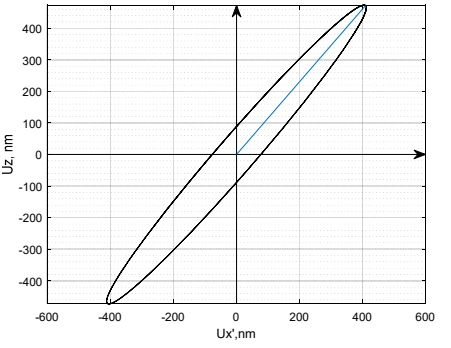

3b) Trajectory of the second contact point (100 V/100 V)

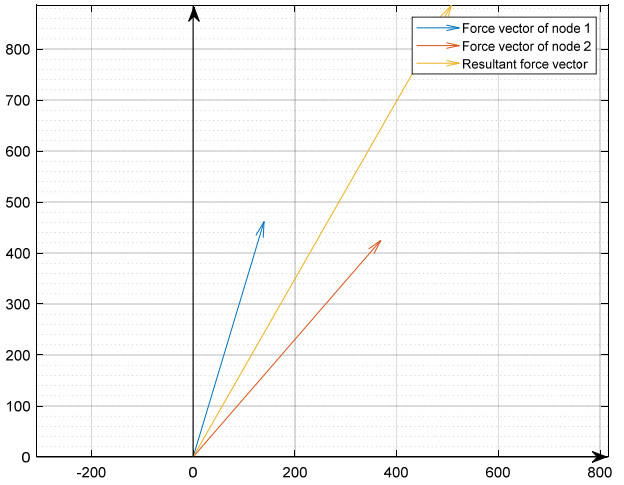

3c) φ =60.1881°, r =1134.6 nm

Fig. A11. Motion trajectories of contact points of a 16 mm × 18.5 mm × 21 mm cylinder with triangular electrode scheme

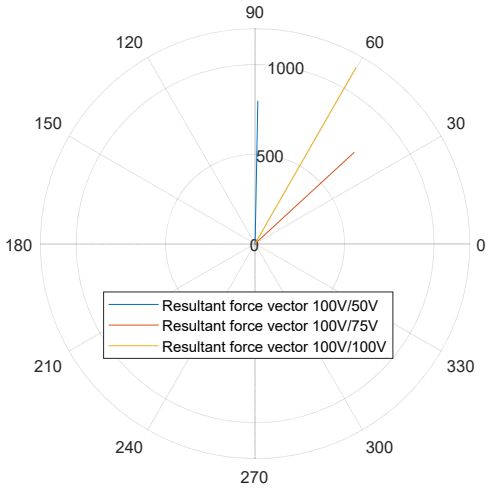

Fig. A12. Resultant force vectors in polar coordinates of contact points of a 16 mm × 18.5 mm × 21 mm cylinder with triangular electrode scheme

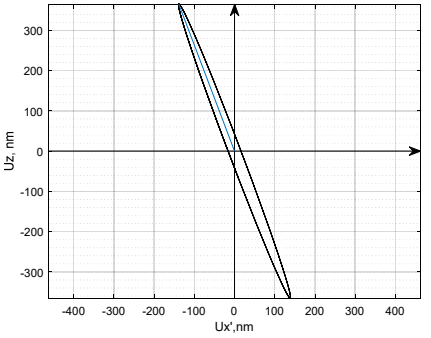

1a) Trajectory of the first contact point (100 V/50 V)

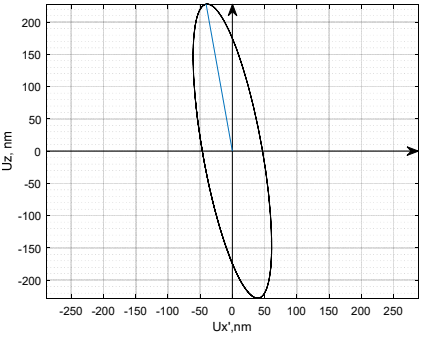

1b) Trajectory of the second contact point (100 V/50 V)

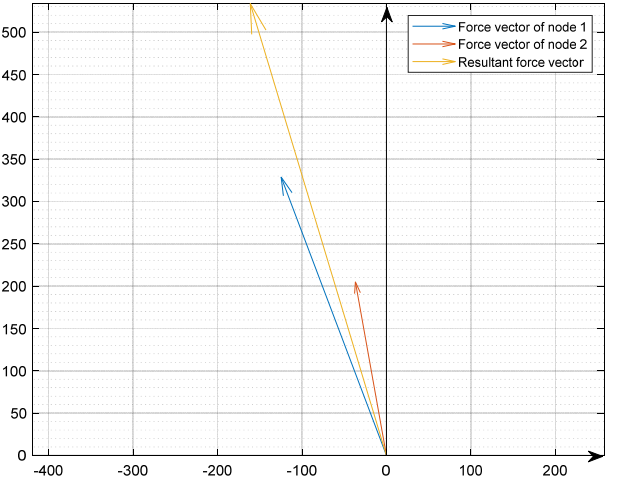

1c) φ =73.1799°, r =619.4291 nm

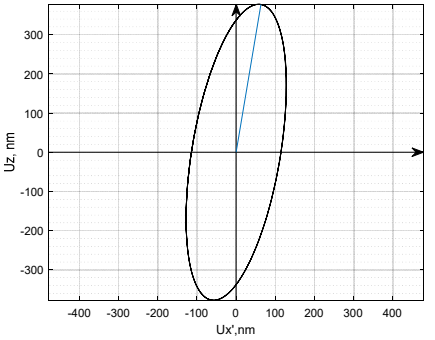

2a) Trajectory of the first contact point (100 V/75 V)

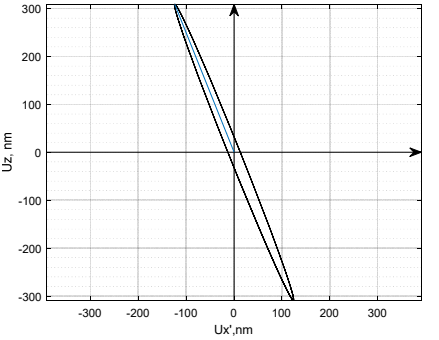

2b) Trajectory of the second contact point (100 V/75 V)

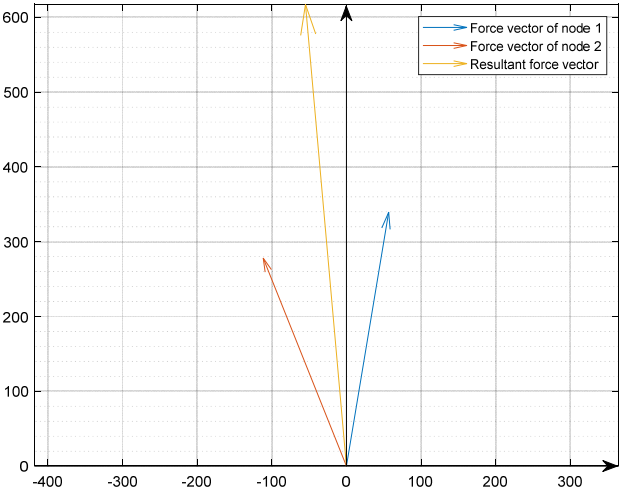

2c) φ =84.9251°, r =688.6428 nm

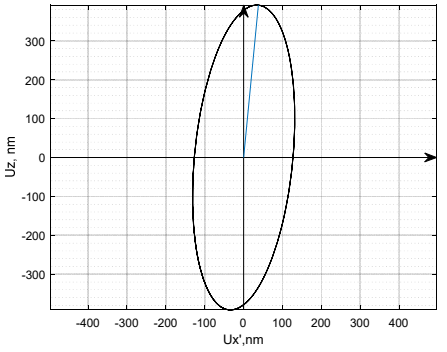

3a) Trajectory of the first contact point (100 V/100 V)

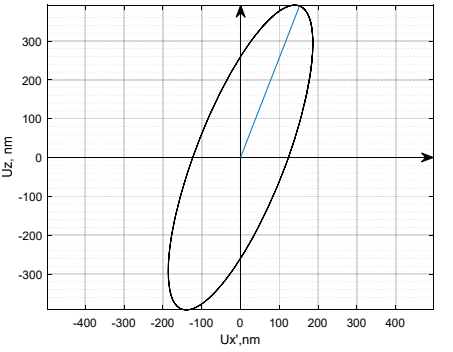

3b) Trajectory of the second contact point (100 V/100 V)

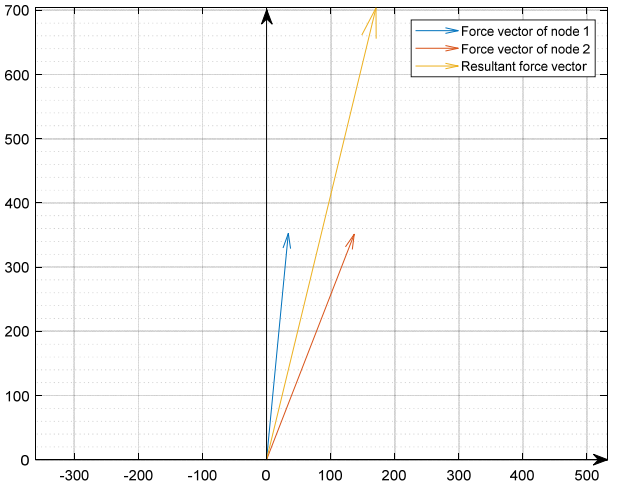

3c) φ =76.3551°, r =804.3359 nm

Fig. A13. Motion trajectories of contact points of an 18 mm × 20.5 mm × 21 mm cylinder with rectangular electrode scheme

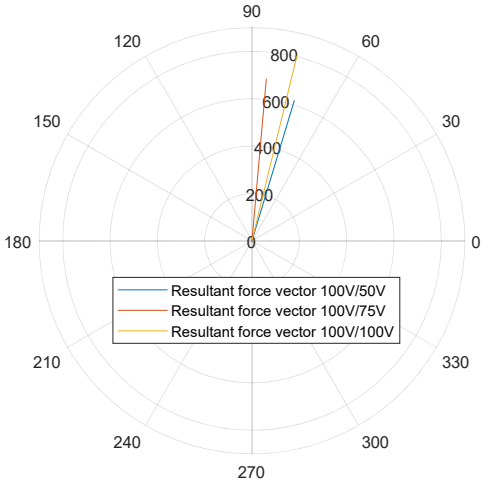

Fig. A14. Resultant force vectors in polar coordinates of contact points of an 18 mm × 20.5 mm × 21 mm cylinder with rectangular electrode scheme

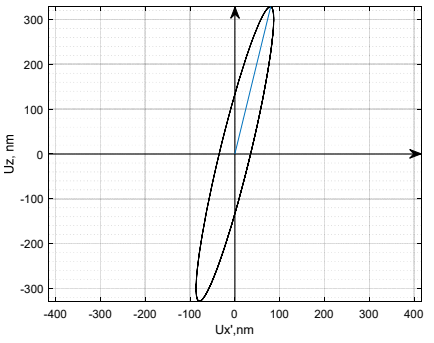

1a) Trajectory of the first contact point (100 V/50 V)

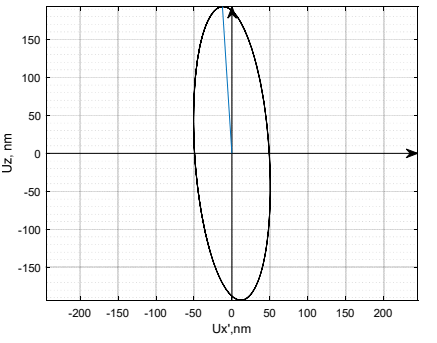

1b) Trajectory of the second contact point (100 V/50 V)

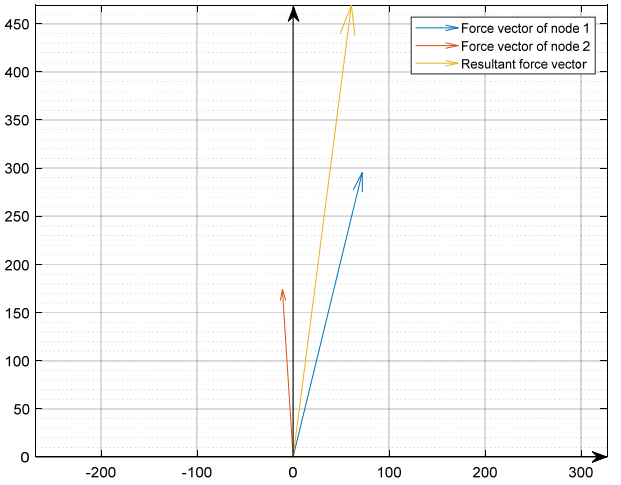

1c) φ =82.6367°, r =525.6410 nm

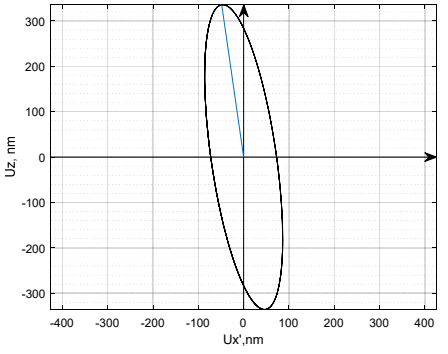

2a) Trajectory of the first contact point (100 V/75 V)

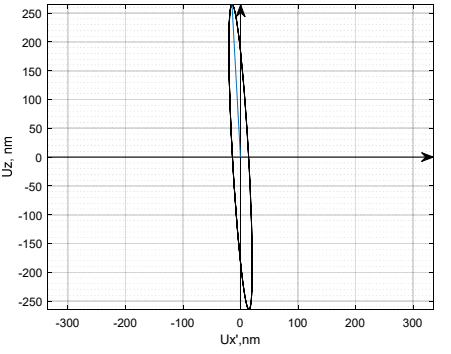

2b) Trajectory of the second contact point (100 V/75 V)

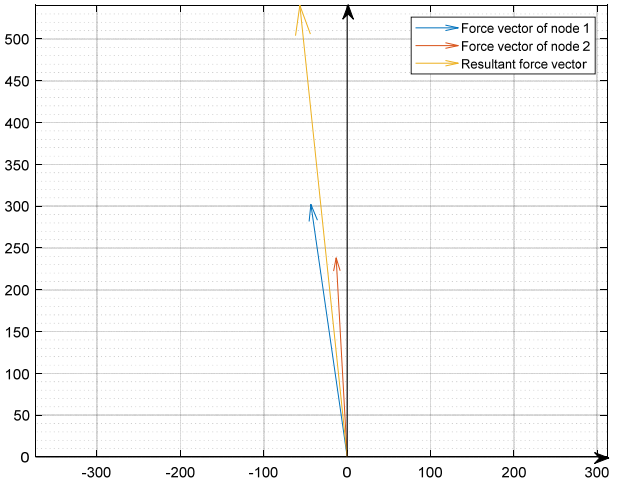

2c) φ =84.0074°, r =603.7382 nm

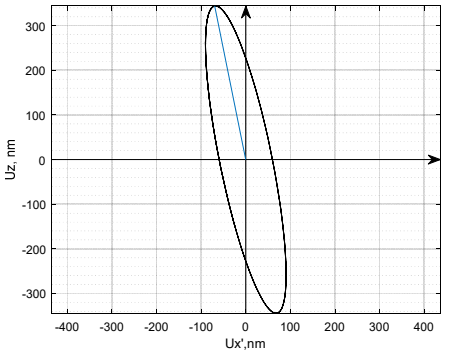

3a) Trajectory of the first contact point (100 V/100 V)

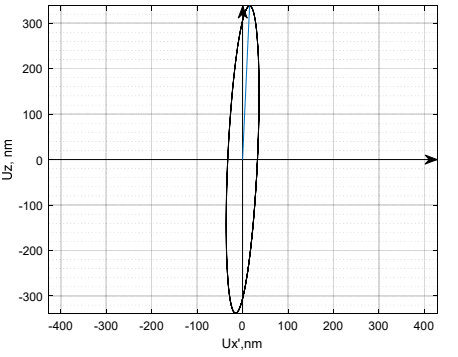

3b) Trajectory of the second contact point (100 V/100 V)

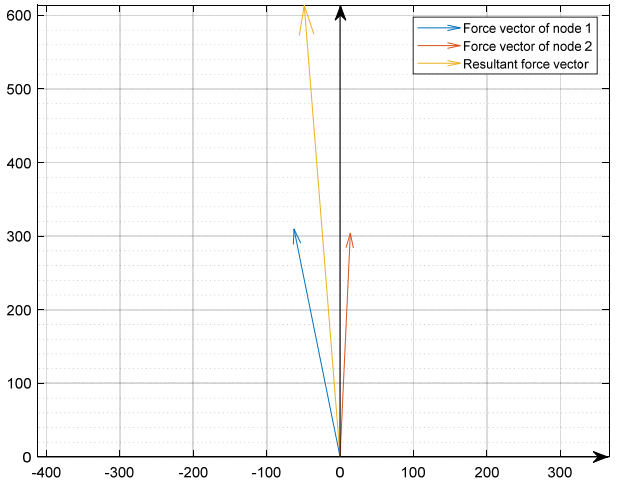

3c) φ =85.4502°, r =684.1352 nm

Fig. A15. Motion trajectories of contact points of an 18 mm × 20.5 mm × 21 mm cylinder with triangular electrode scheme

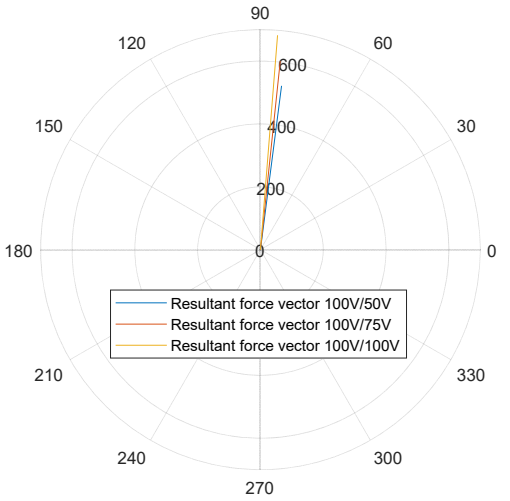

Fig. A16. Resultant force vectors in polar coordinates of contact points of an 18 mm × 20.5 mm × 21 mm cylinder with triangular electrode scheme

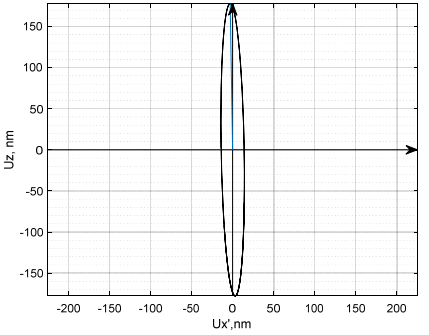

1a) Trajectory of the first contact point (100 V/50 V)

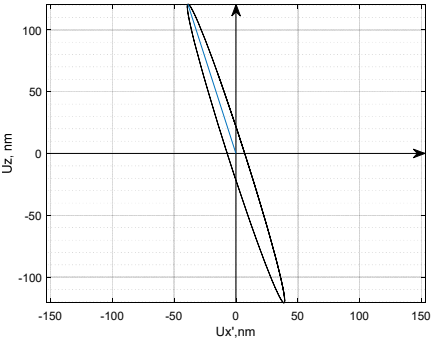

1b) Trajectory of the second contact point (100 V/50 V)

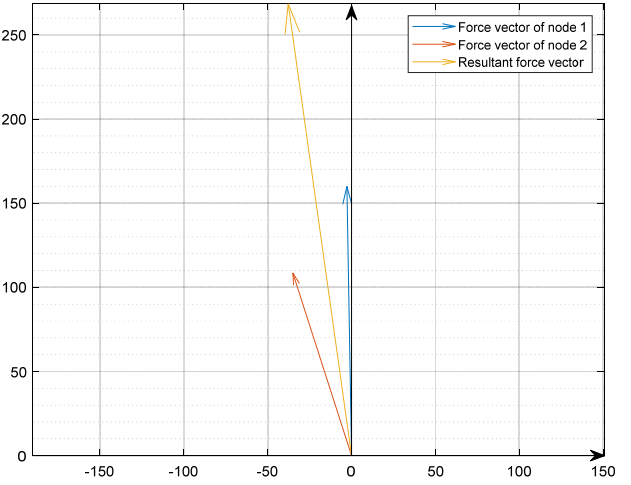

1c) φ =82.0094°, r =301.2906 nm

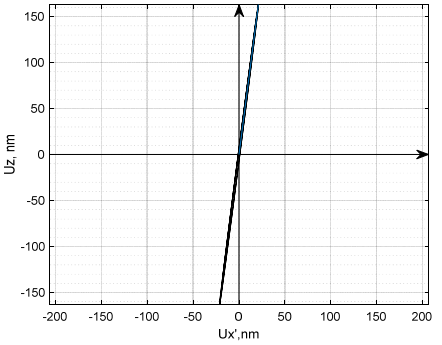

2a) Trajectory of the first contact point (100 V/75 V)

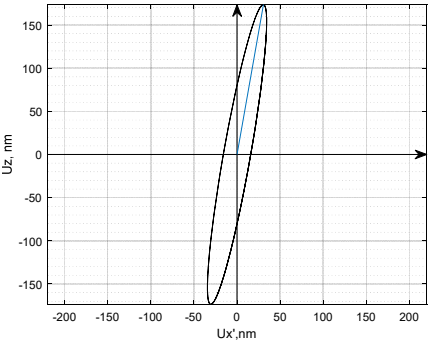

2b) Trajectory of the second contact point (100 V/75 V)

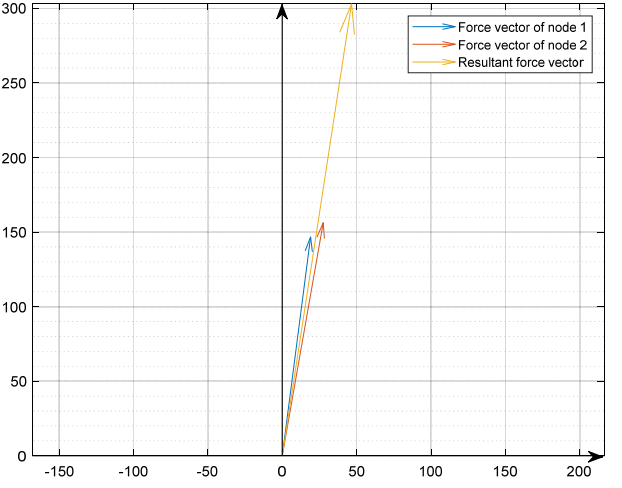

2c) φ =81.2543°, r =340.5799 nm

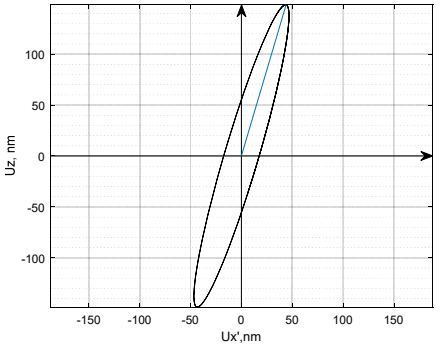

3a) Trajectory of the first contact point (100 V/100 V)

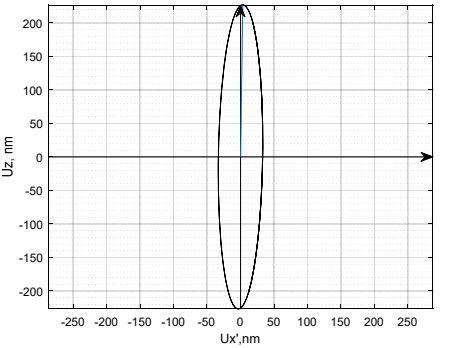

3b) Trajectory of the second contact point (100 V/100 V)

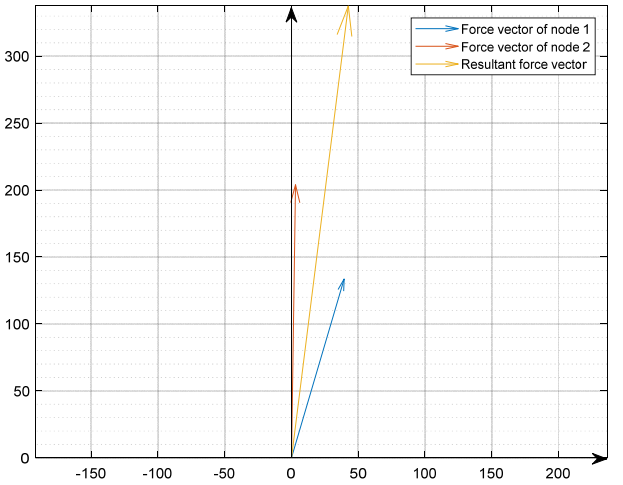

3c) φ =82.8181°, r =377.9811 nm

Fig. A17. Motion trajectories of contact points of a 10 mm × 12.5 mm × 23 mm cylinder with rectangular electrode scheme

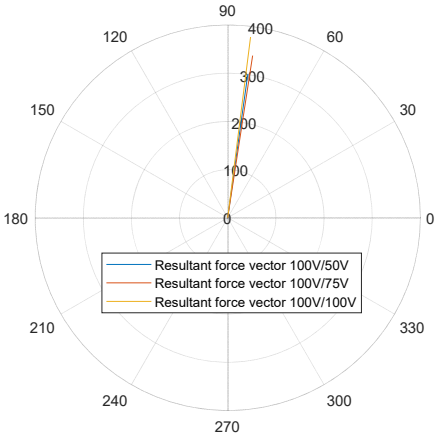

Fig. A18. Resultant force vectors in polar coordinates of contact points of a 10 mm × 12.5 mm × 23 mm cylinder with rectangular electrode scheme

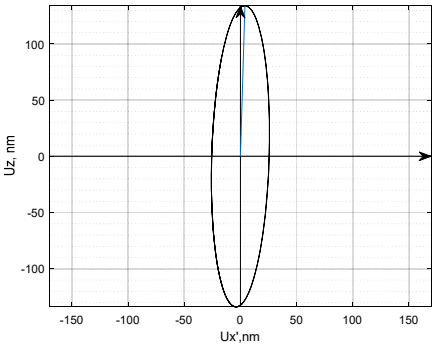

1a) Trajectory of the first contact point (100 V/50 V)

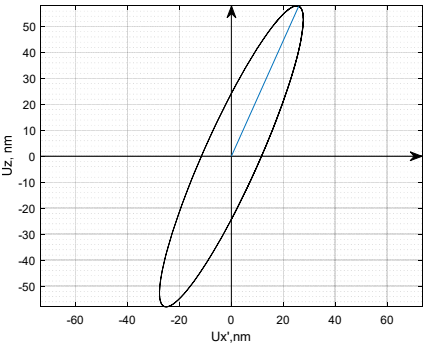

1b) Trajectory of the second contact point (100 V/50 V)

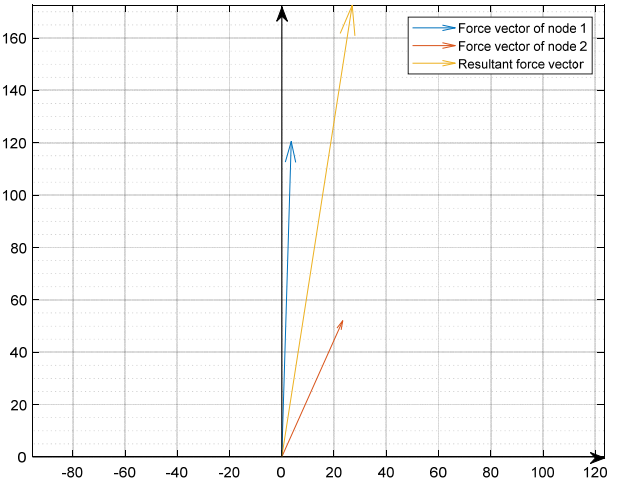

1c) φ =81.1114°, r =94.0051 nm

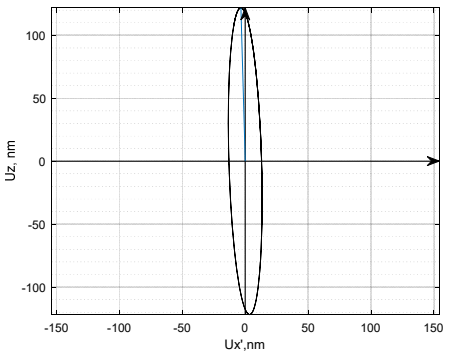

2a) Trajectory of the first contact point (100 V/75 V)

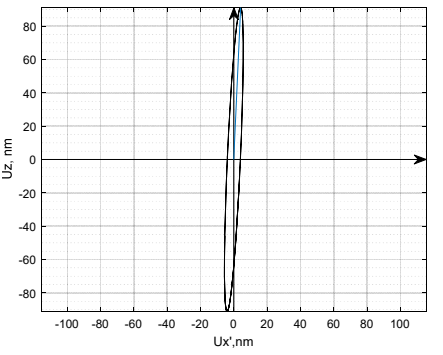

2b) Trajectory of the second contact point (100 V/75 V)

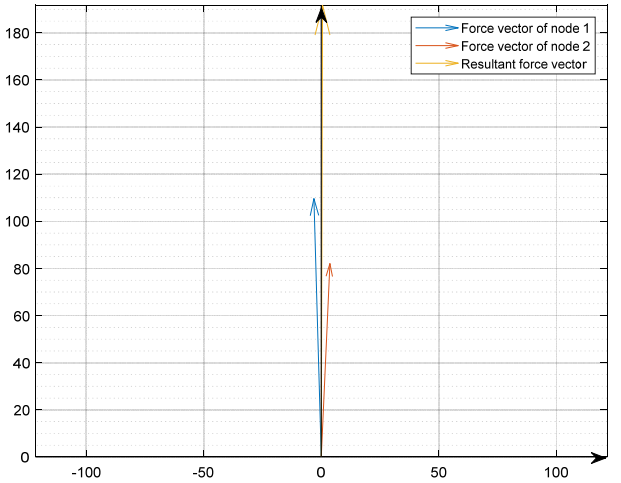

2c) φ =89.8493°, r =212.9873 nm

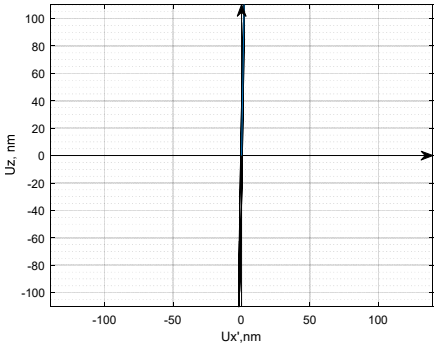

3a) Trajectory of the first contact point (100 V/100 V)

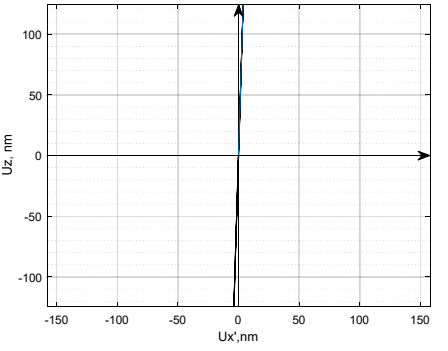

3b) Trajectory of the second contact point (100 V/100 V)

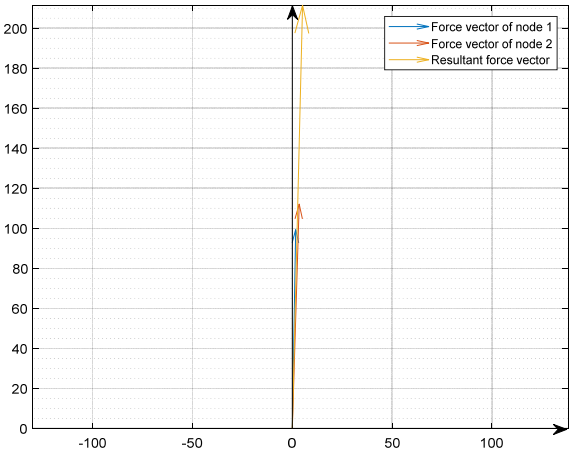

3c) φ =88.5991°, r =234.9532 nm

Fig. A19. Motion trajectories of contact points of a 10 mm × 12.5 mm × 23 mm cylinder with triangular electrode scheme

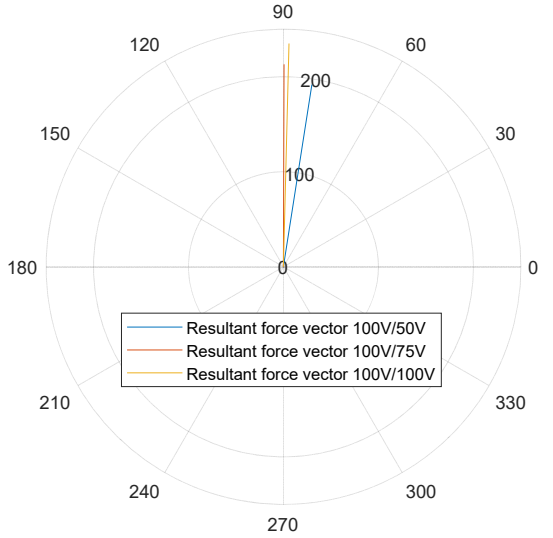

Fig. A20. Resultant force vectors in polar coordinates of contact points of a 10 mm × 12.5 mm × 23 mm cylinder with triangular electrode scheme

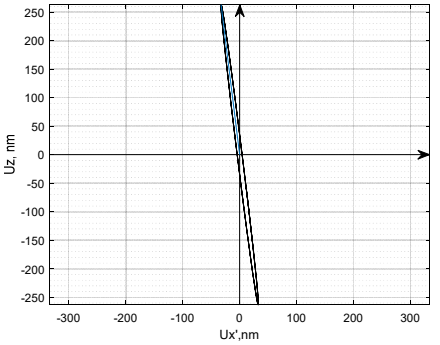

1a) Trajectory of the first contact point (100 V/50 V)

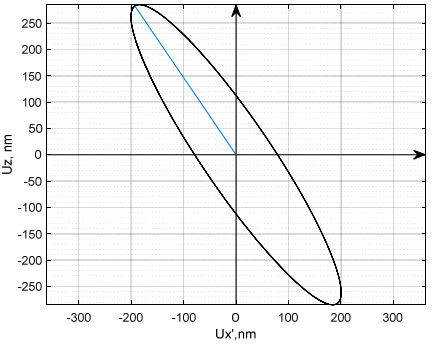

1b) Trajectory of the second contact point (100 V/50 V)

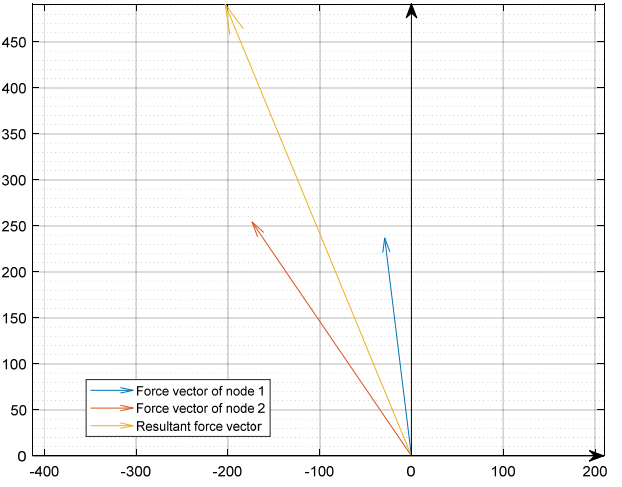

1c) φ =67.5492°, r =590.3938 nm

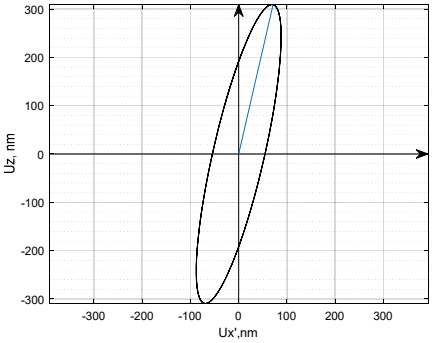

2a) Trajectory of the first contact point (100 V/75 V)

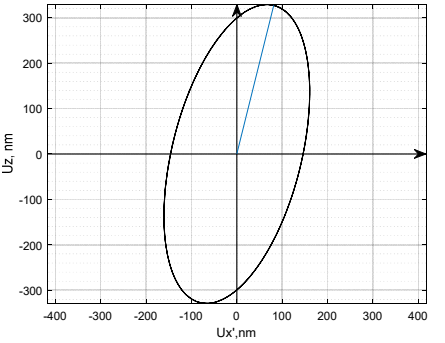

2b) Trajectory of the second contact point (100 V/75 V)

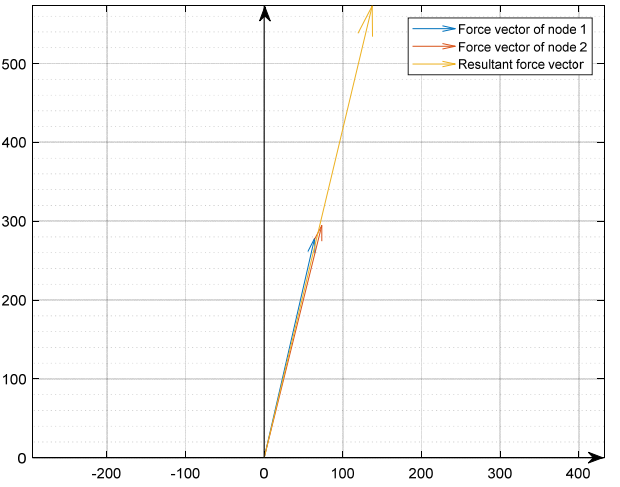

2c) φ =76.5355°, r =654.6003 nm

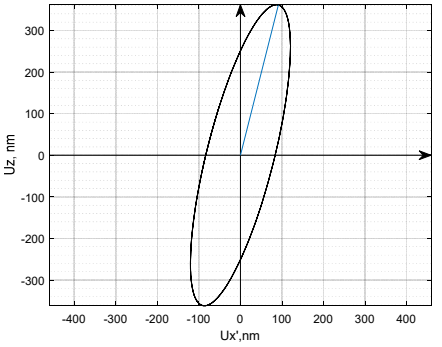

3a) Trajectory of the first contact point (100 V/100 V)

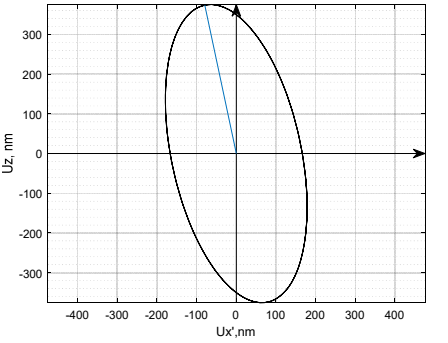

3b) Trajectory of the second contact point (100 V/100 V)

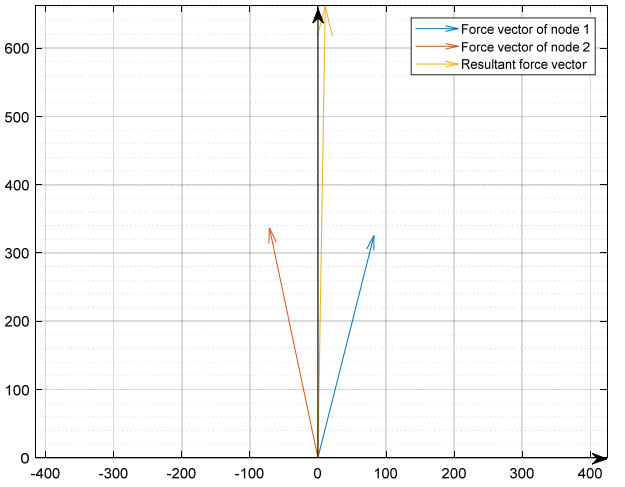

3c) φ =89.0614°, r =735.3459 nm

Fig. A21. Motion trajectories of contact points of a 12 mm × 14.5 mm × 23 mm cylinder with rectangular electrode scheme

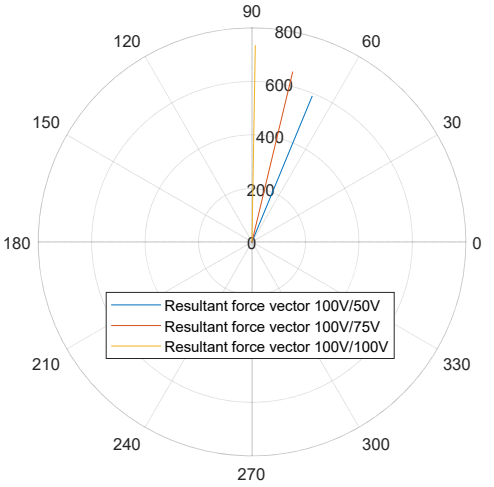

Fig. A22. Resultant force vectors in polar coordinates of contact points of a 12 mm × 14.5 mm × 23 mm cylinder with rectangular electrode scheme

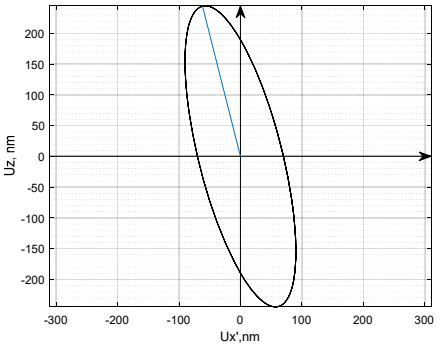

1a) Trajectory of the first contact point (100V/50V)

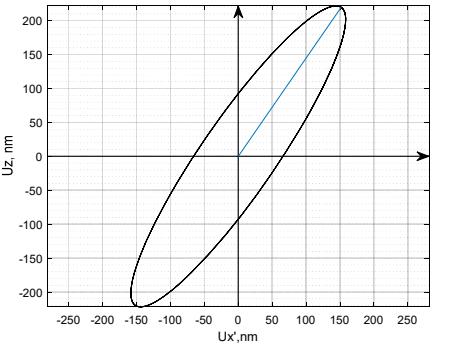

1b) Trajectory of the second contact point (100V/50V)

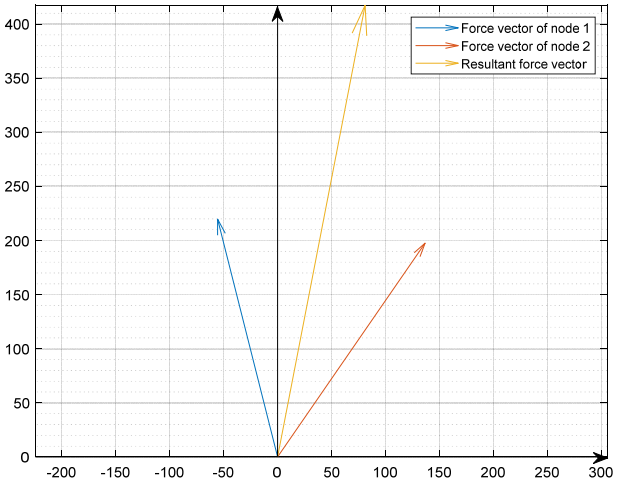

1c) φ =79.0044°, r =472.4261 nm

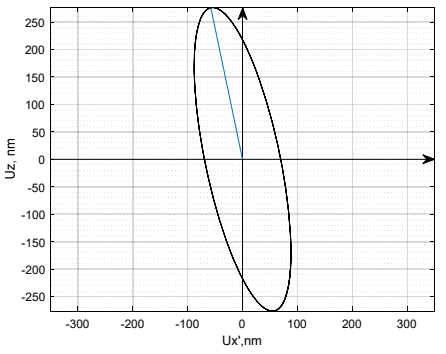

2a) Trajectory of the first contact point (100 V/75 V)

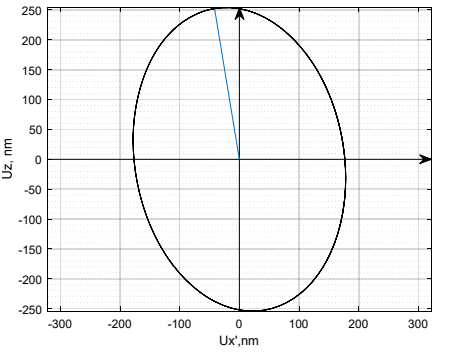

2b) Trajectory of the second contact point (100 V/75 V)

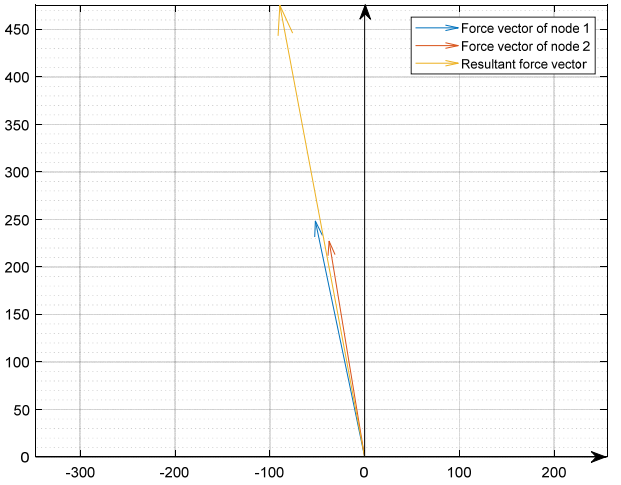

2c) φ =79.3551°, r =537.5404 nm

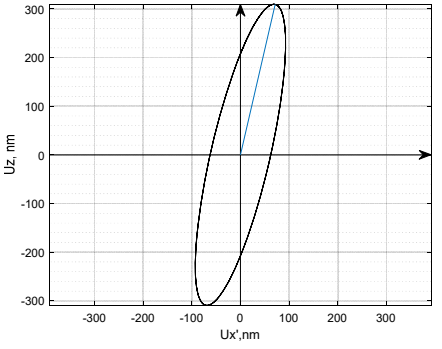

3a) Trajectory of the first contact point (100 V/100 V)

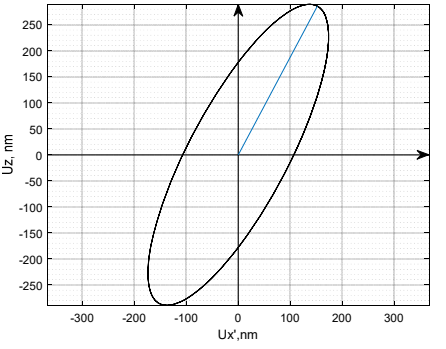

3b) Trajectory of the second contact point (100 V/100 V)

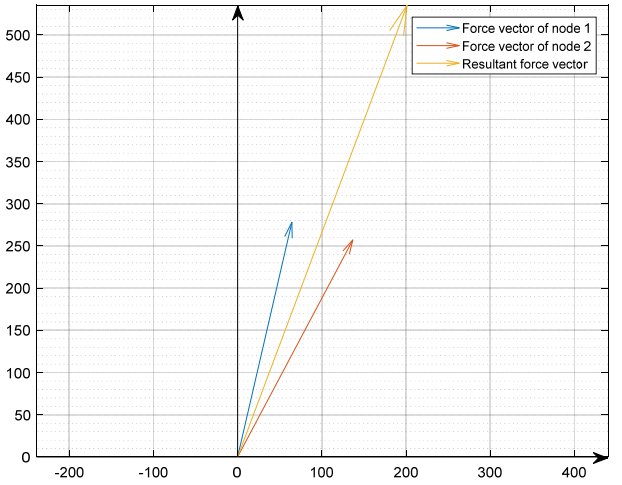

3c) φ =69.3972°, r =635.3427 nm

Fig. A23. Motion trajectories of contact points of a 12 mm × 14.5 mm × 23 mm cylinder with triangular electrode scheme

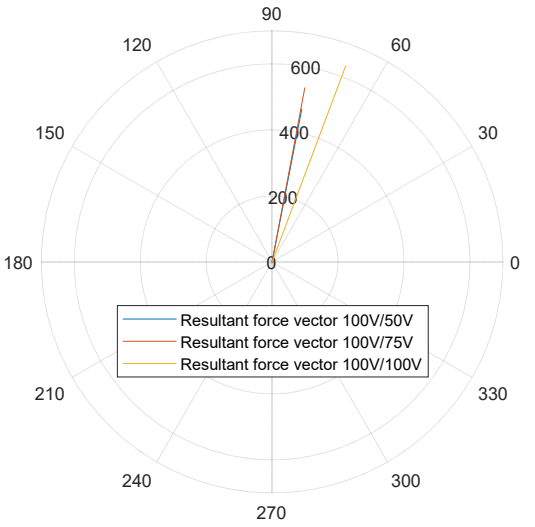

Fig. A24. Resultant force vectors in polar coordinates of contact points of a 12 mm × 14.5 mm × 23 mm cylinder with triangular electrode scheme

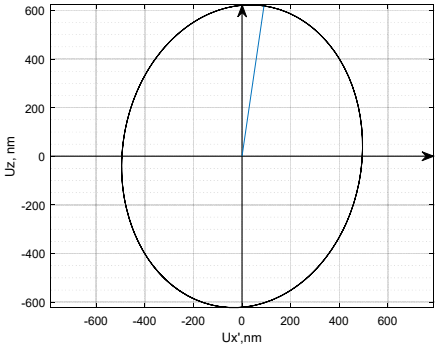

1a) Trajectory of the first contact point (100 V/50 V)

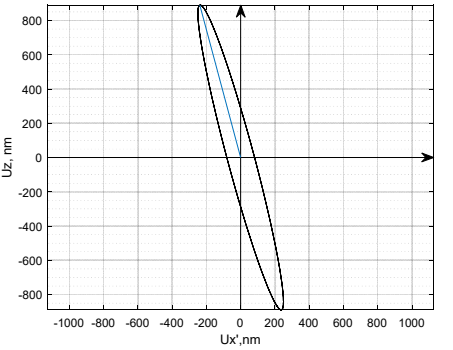

1b) Trajectory of the second contact point (100 V/50 V)

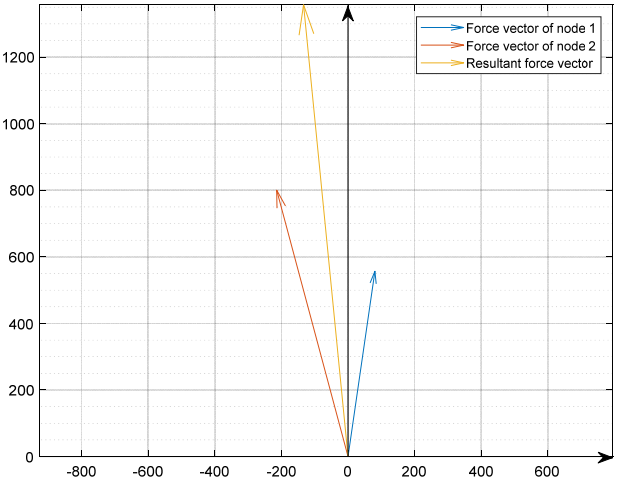

1c) $\varphi = 84.3799°$, $r = 1515$ nm

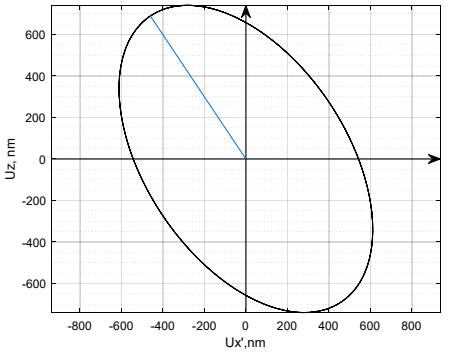

2a) Trajectory of the first contact point (100 V/75 V)

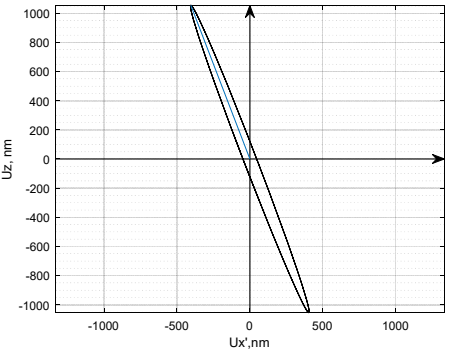

2b) Trajectory of the second contact point (100 V/75 V)

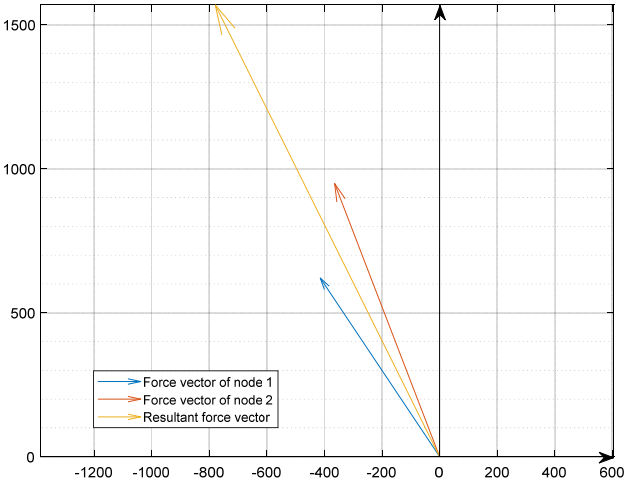

2c) $\varphi = 63.6004°, r = 1946.5$ nm

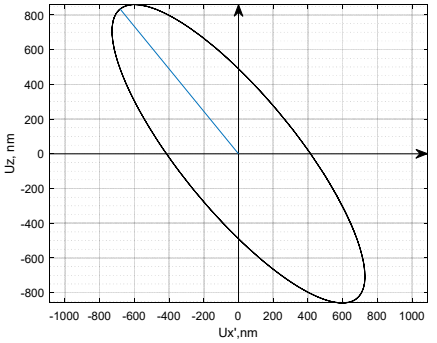

3a) Trajectory of the first contact point (100V/100V)

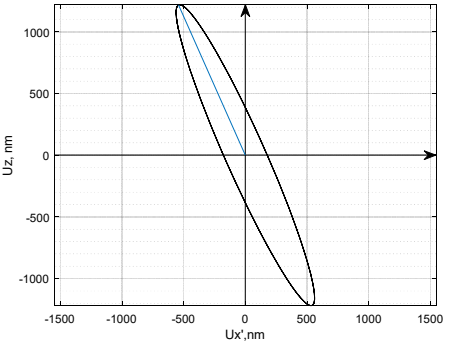

3a) Trajectory of the first contact point (100V/100V)

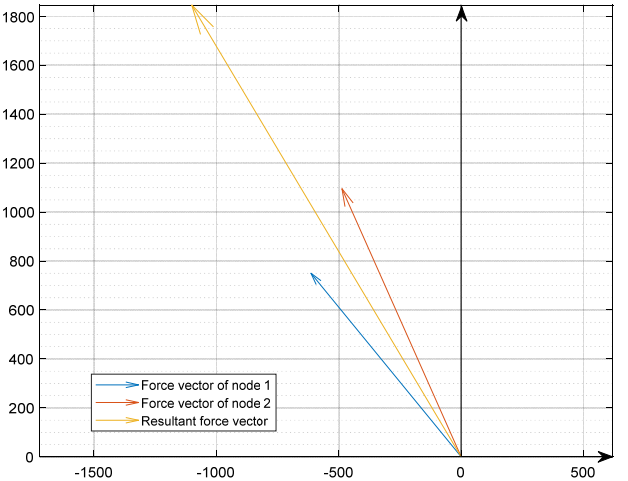

3c) $\varphi = 59.2002°, r = 2388.2$ nm

Fig. A25. Motion trajectories of contact points of a 14 mm × 16.5 mm × 23 mm cylinder with rectangular electrode scheme

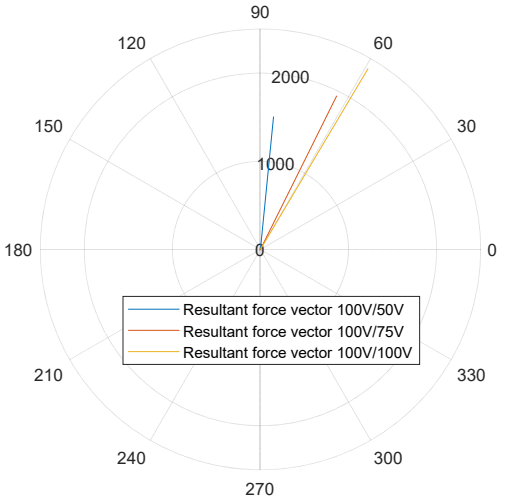

Fig. A26. Resultant force vectors in polar coordinates of contact points of a 14 mm × 16.5 mm × 23 mm cylinder with rectangular electrode scheme

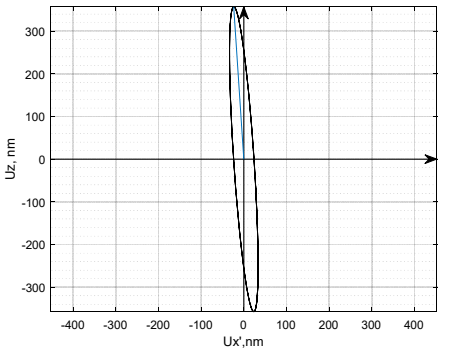

1a) Trajectory of the first contact point (100 V/50 V)

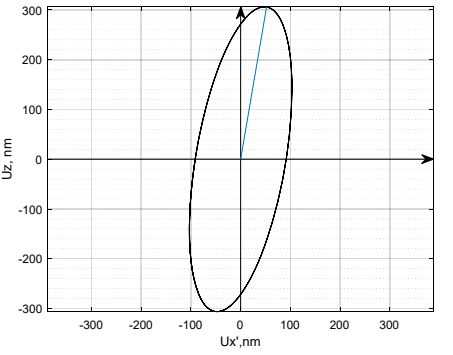

1b) Trajectory of the second contact point (100 V/50 V)

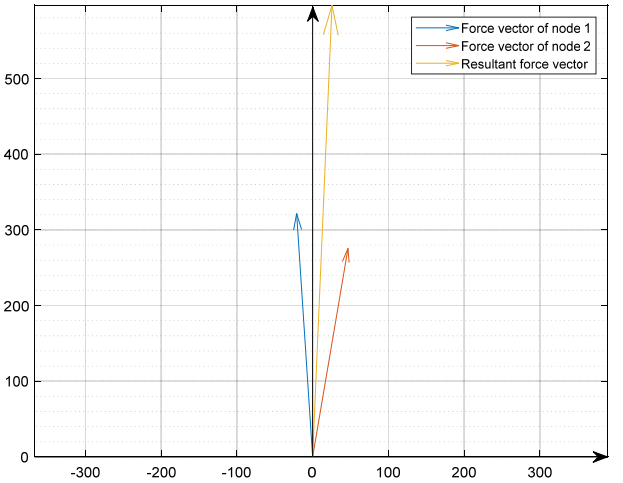

1c) $\varphi = 87.5451°, r = 663.6917$ nm

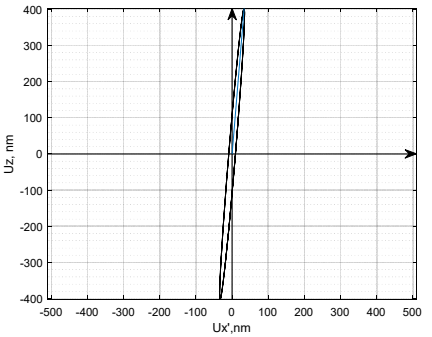

2a) Trajectory of the first contact point (100 V/75 V)

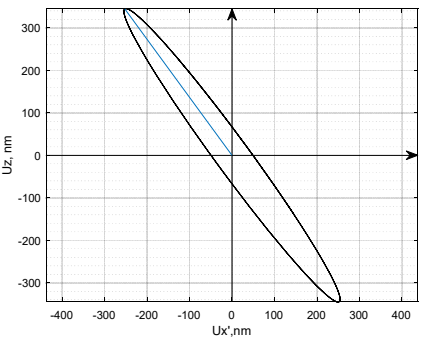

2b) Trajectory of the second contact point (100 V/75 V)

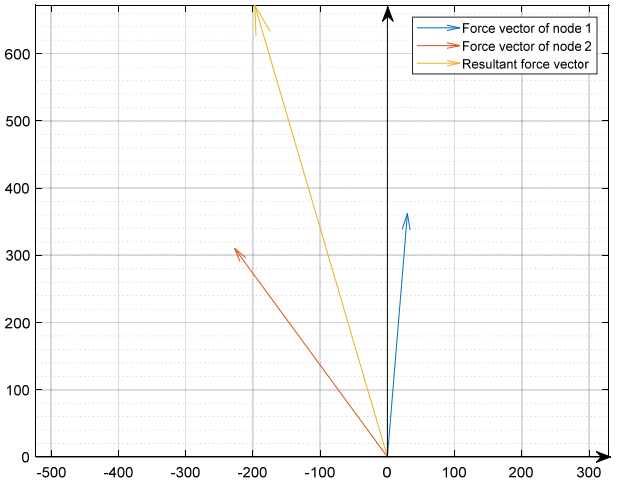

2c) $\varphi = 73.6396°, r = 778.1933$ nm

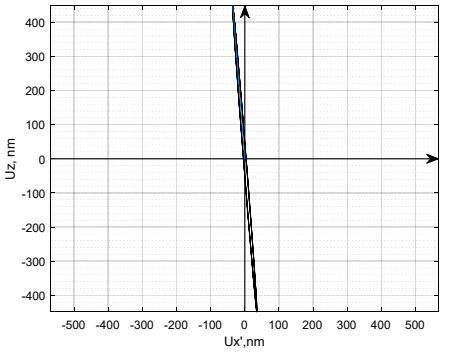

3a) Trajectory of the first contact point (100 V/100 V)

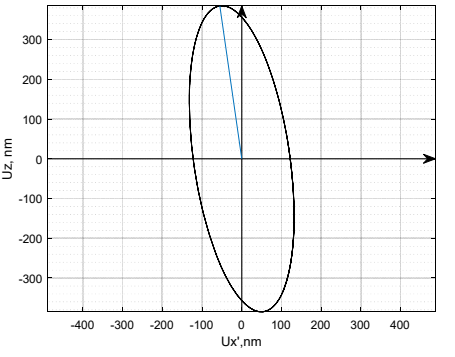

3a) Trajectory of the first contact point (100 V/100 V)

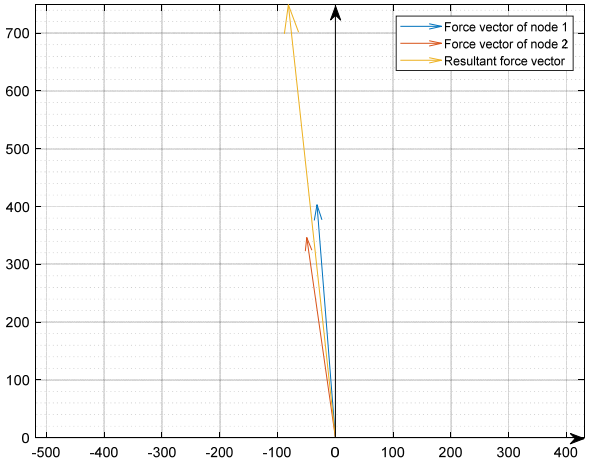

3c) $\varphi = 83.8096°, r = 837.5139$ nm

Fig. A27. Motion trajectories of contact points of a 14 mm × 16.5 mm × 23 mm cylinder with triangular electrode scheme

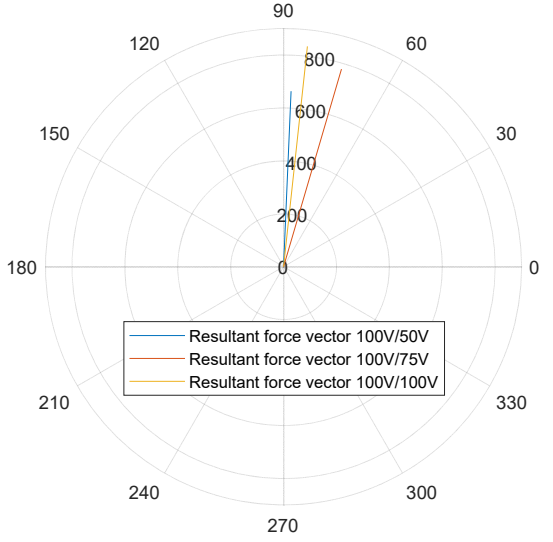

Fig. A28. Resultant force vectors in polar coordinates of contact points of a 14 mm × 16.5 mm × 23 mm cylinder with triangular electrode scheme

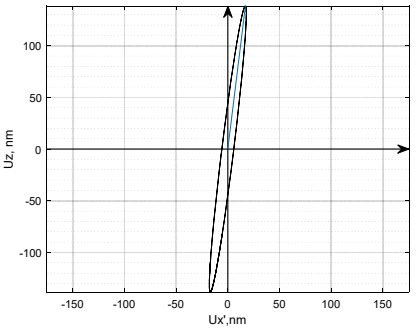

1a) Trajectory of the first contact point (100 V/50 V)

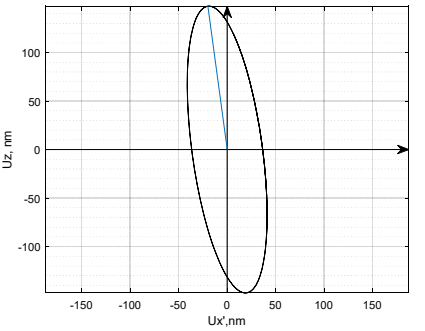

1b) Trajectory of the second contact point (100 V/50 V)

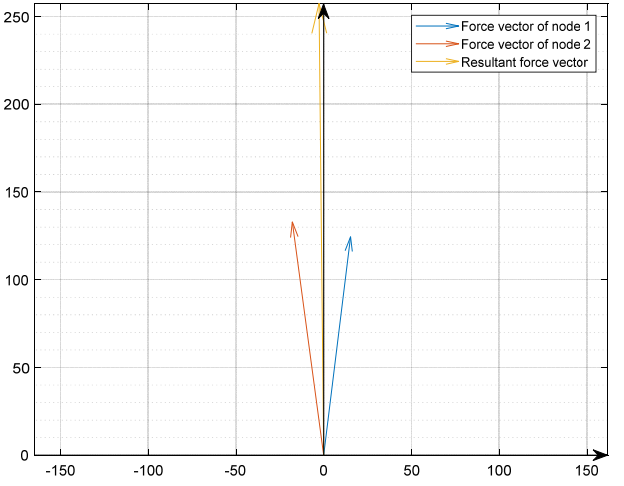

1c) $\varphi = 89.3960°$, $r = 286.0665$ nm

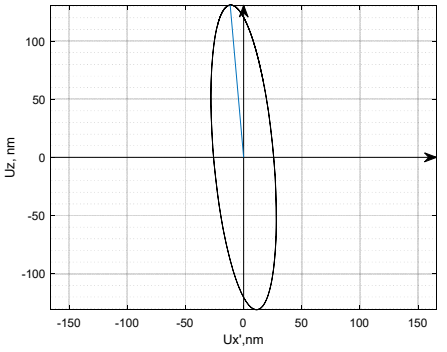

2a) Trajectory of the first contact point (100 V/75 V)

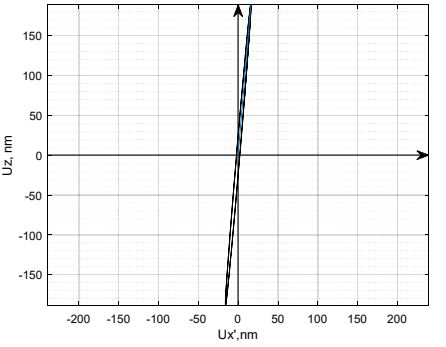

2b) Trajectory of the second contact point (100 V/75 V)

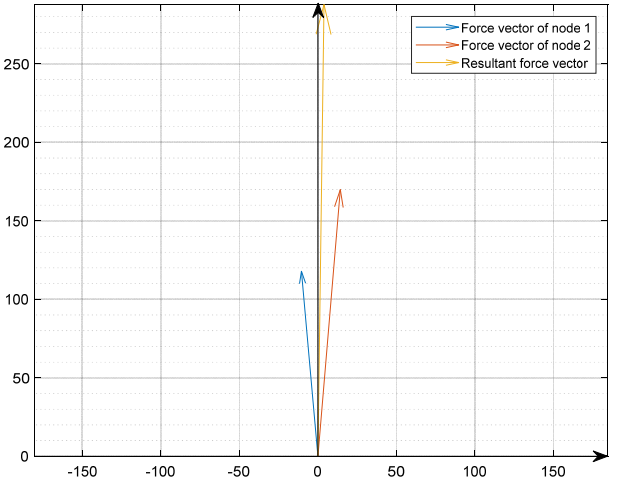

2c) $\varphi = 89.2219°, r = 319.6857$ nm

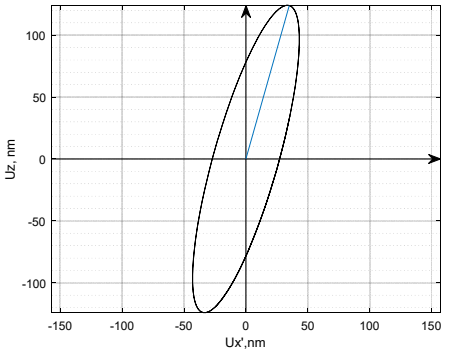

3a) Trajectory of the first contact point (100 V/100 V)

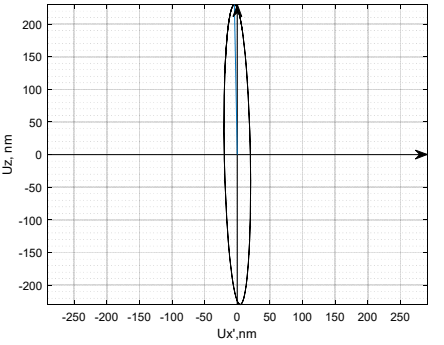

3a) Trajectory of the first contact point (100 V/100 V)

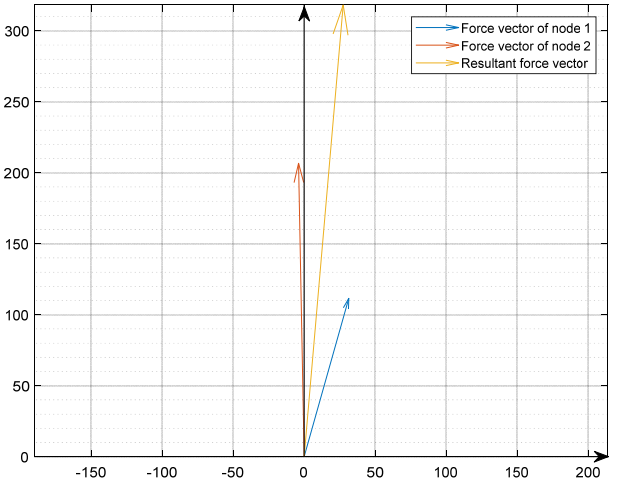

3c) $\varphi = 85.0588°$, $r = 354.9454$ nm

Fig. A29. Motion trajectories of contact points of a 10 mm × 12.5 mm × 25 mm cylinder with rectangular electrode scheme

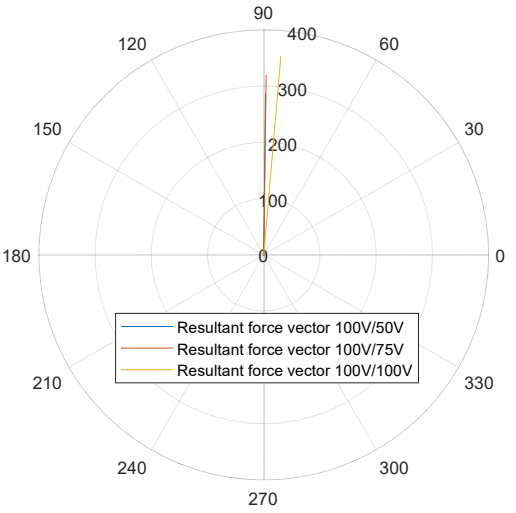

Fig. A30. Resultant force vectors in polar coordinates of contact points of a 10 mm × 12.5 mm × 25 mm cylinder with rectangular electrode scheme

Table A1. Domination coefficients, cylinder PZT-4.

Geometrical parameters($r \times R \times h$)	**Values of domination coefficients**	
18 mm × 20.5 mm × 21 mm	m_1^n =0.187494 m_2^n =0.210533 m_3^n =0.601973 N=89	m_1^n =0.371500 m_2^n =0.137957 m_3^n =0.490543 N=95
	m_1^n =0.467842 m_2^n =0.156221 m_3^n =0.375938 N=89	
10 mm × 12.5 mm × 23 mm	m_1^n =0.387297 m_2^n =0.171246 m_3^n =0.441456 N=33	m_1^n =0.153420 m_2^n =0.391514 m_3^n =0.455066 N=53
	m_1^n =0.604846 m_2^n =0.173869 m_3^n =0.221285 N=58	m_1^n =0.045906 m_2^n =0.099334 m_3^n =0.854760 N=61
18 mm × 20.5 mm × 23 mm	m_1^n =0.460868 m_2^n =0.461369 m_3^n =0.077764 N=43	m_1^n =0.235397 m_2^n =0.413286 m_3^n =0.351316 N=83
	m_1^n =0.360716 m_2^n =0.145903 m_3^n =0.493382 N=86	

A.2. Contact point trajectories of the hemispheric piezorobot

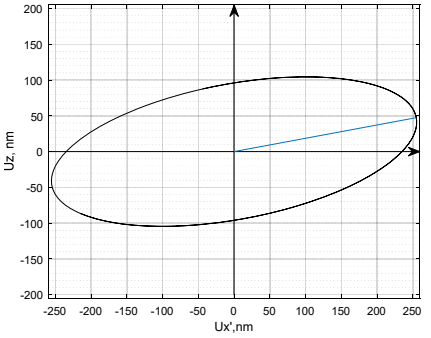

1a) Trajectory of the first contact point (100 V/50 V)

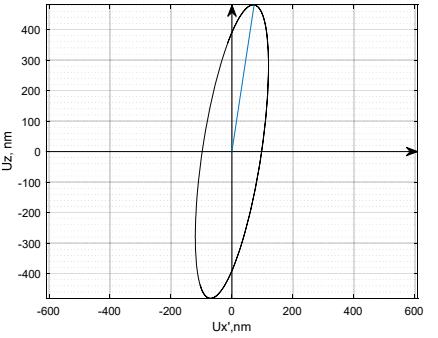

1b) Trajectory of the second contact point (100 V/50 V)

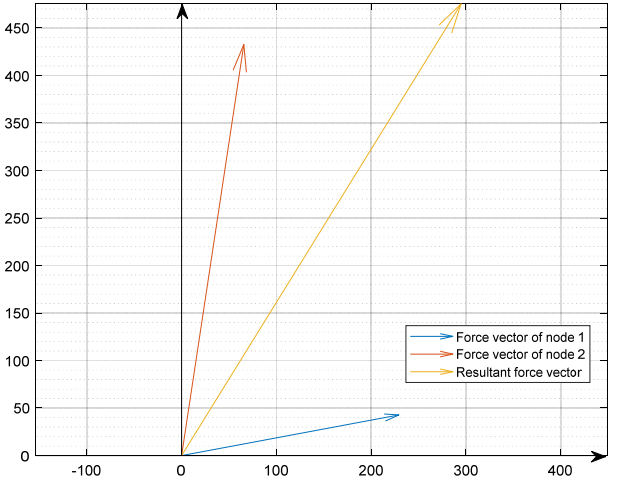

1c) φ =55.7223°, r =581.8081 nm

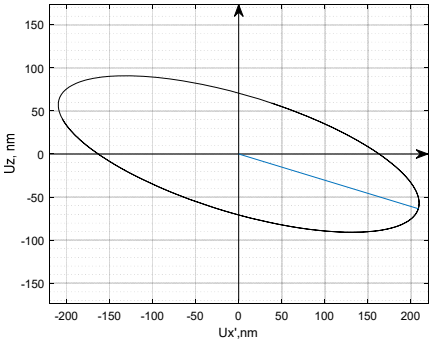

2a) Trajectory of the first contact point (100 V/75 V)

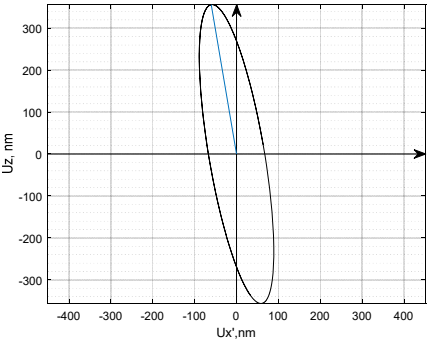

2b) Trajectory of the second contact point (100 V/75 V)

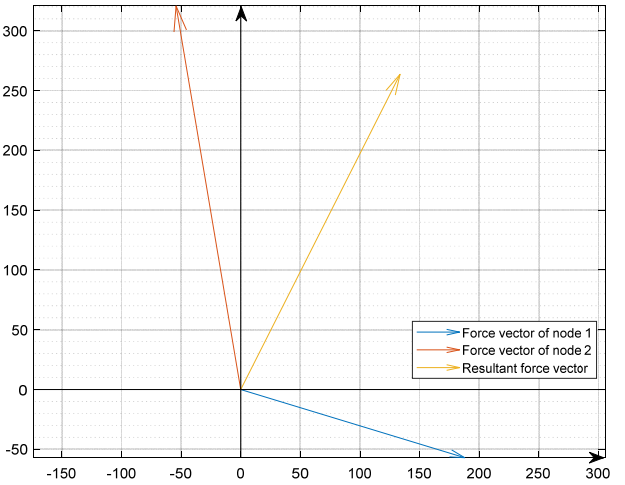

2c) φ =63.1313°, r =328.3822 nm

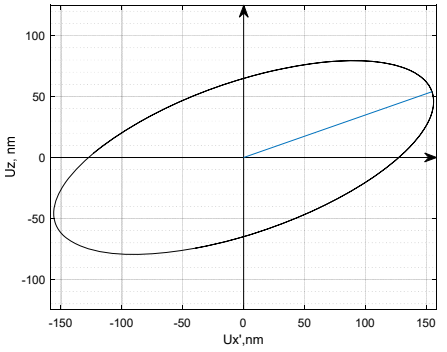

3a) Trajectory of the first contact point (100 V/100 V)

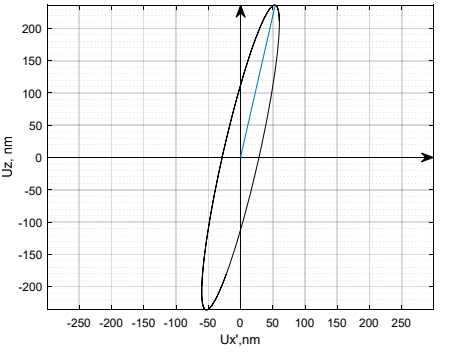

3b) Trajectory of the second contact point (100 V/100 V)

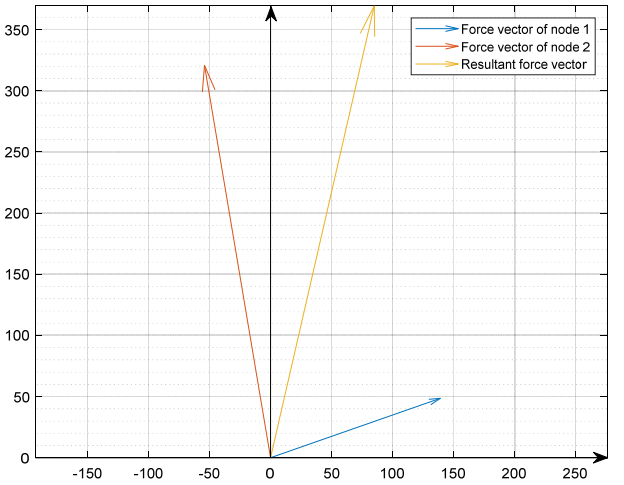

3c) φ =54.3169°, r =356.9252 nm

Fig. A28. Motion trajectories of contact points of a 11.5 mm × 13 mm × 13 mm hemisphere

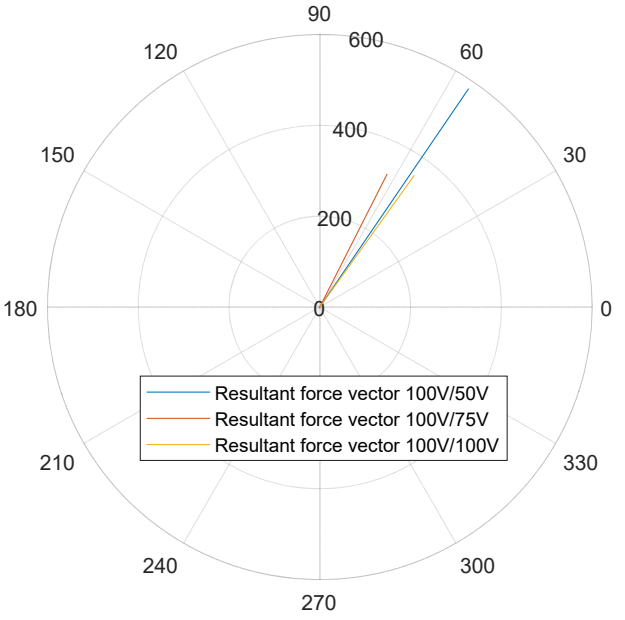

Fig. A29. Resultant force vectors in polar coordinates of contact points of a 11.5 mm × 13 mm × 13 mm hemisphere

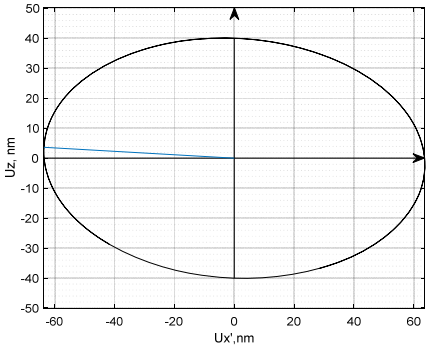

1a) Trajectory of the first contact point (100 V/50 V)

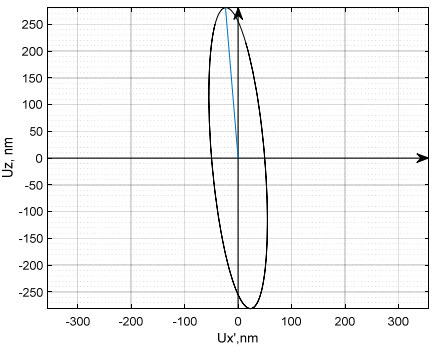

1b) Trajectory of the second contact point (100 V/50 V)

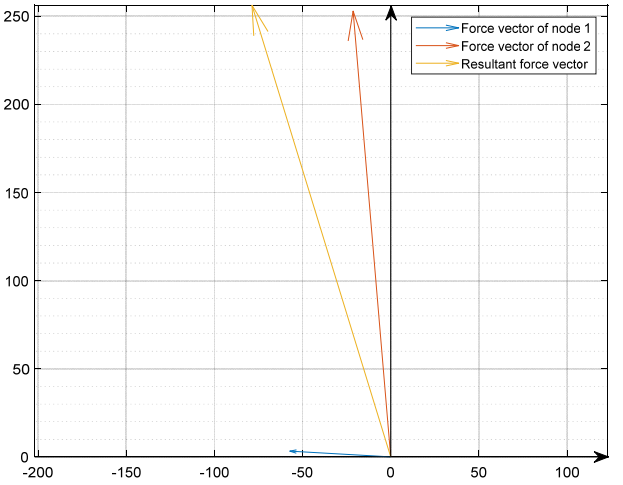

1c) φ =80.9379°, r =247.7817 nm

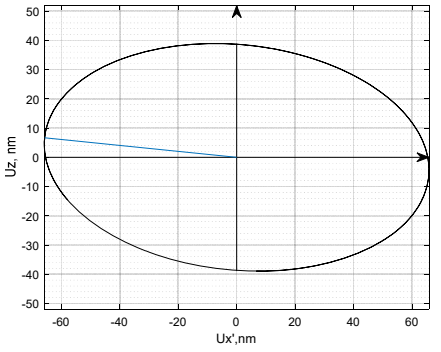

2a) Trajectory of the first contact point (100 V/75 V)

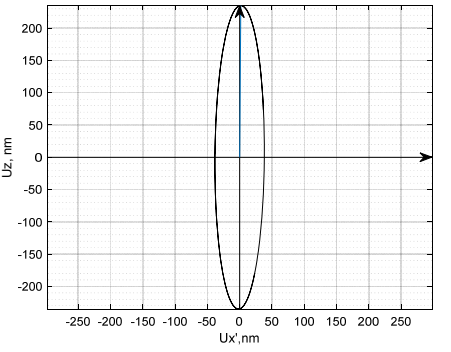

2b) Trajectory of the second contact point (100 V/75 V)

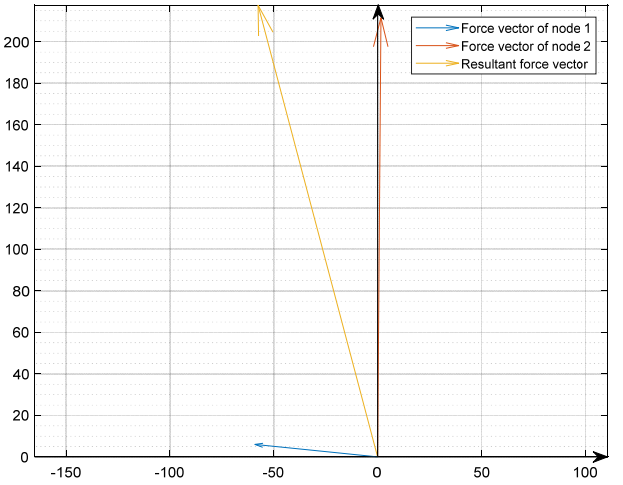

2c) φ =79.0811°, r =411.9999 nm

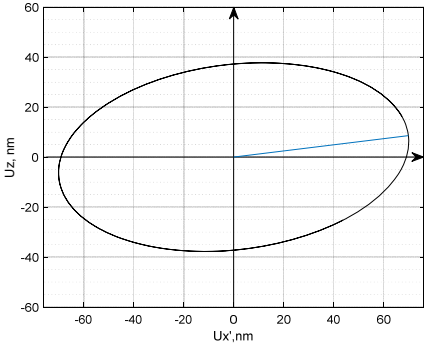

3a) Trajectory of the first contact point (100 V/100 V)

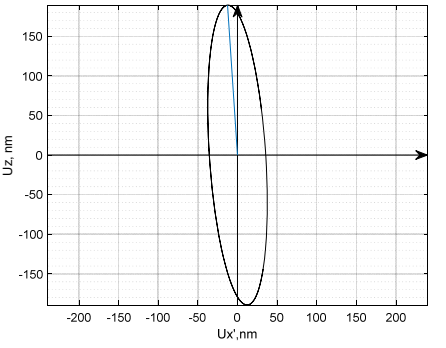

3b) Trajectory of the second contact point (100 V/100 V)

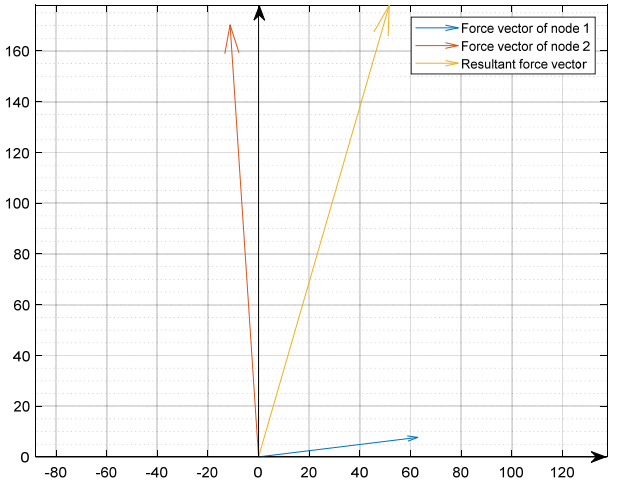

3c) φ =78.72°, r = 456.1667 nm

Fig. A30. Motion trajectories of contact points of a 11.5 mm × 13 mm × 11 mm hemisphere

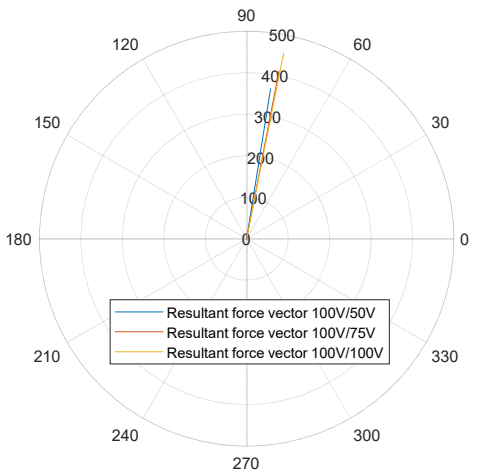

Fig. A31. Resultant force vectors in polar coordinates of contact points of a 11.5 mm × 13 mm × 11 mm hemisphere

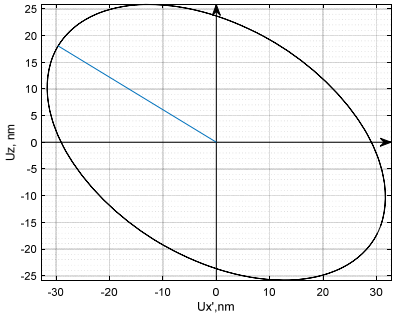

1a) Trajectory of the first contact point (100 V/50 V)

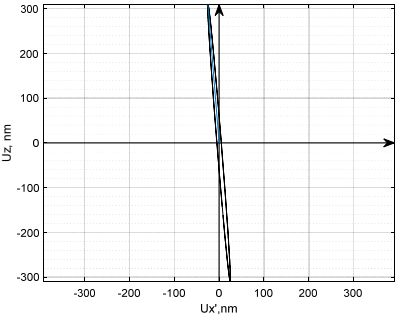

1b) Trajectory of the second contact point (100 V/50 V)

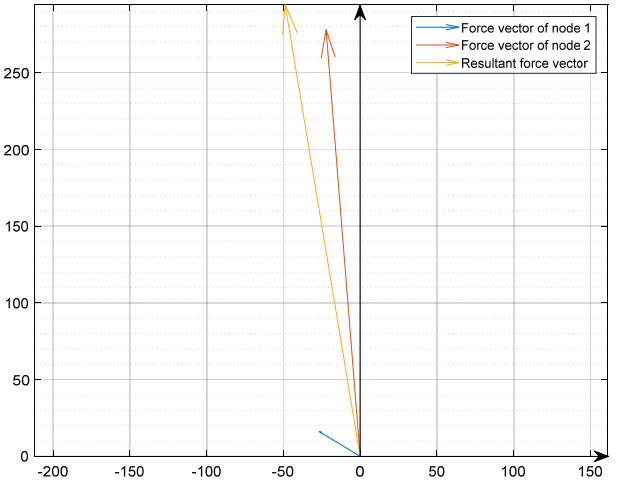

1c) φ =80.56°, r = 331.5494 nm

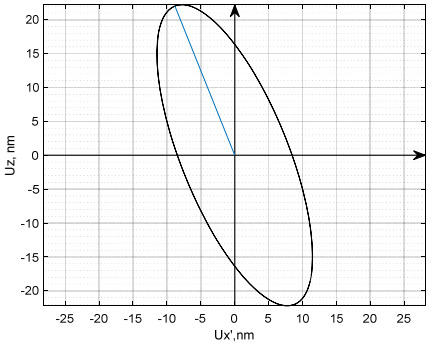

2a) Trajectory of the first contact point (100 V/75 V)

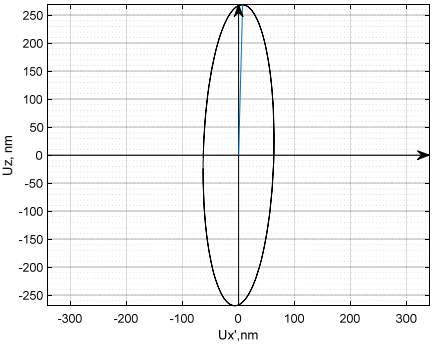

2b) Trajectory of the second contact point (100 V/75 V)

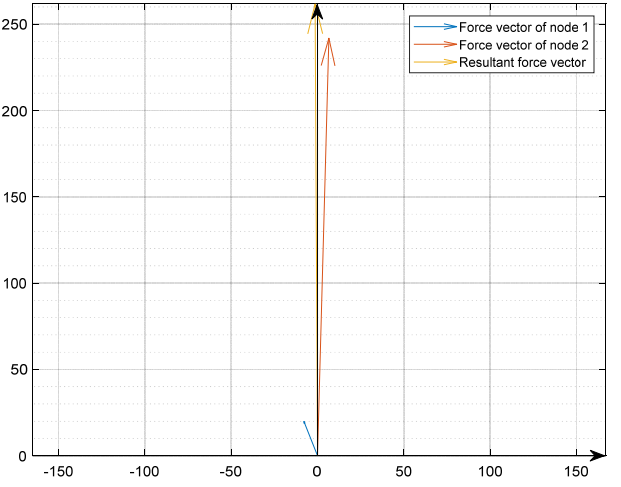

2c) $\varphi = 89.6857°$, $r = 290.7534$ nm

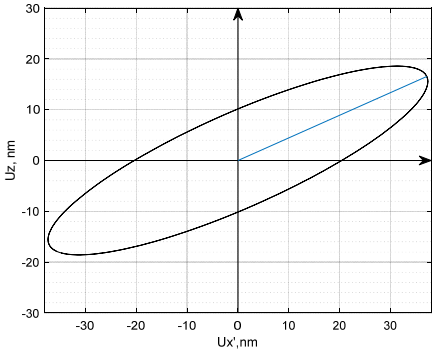

3a) Trajectory of the first contact point (100 V/100 V)

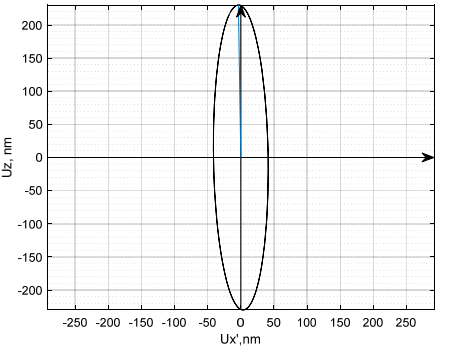

3b) Trajectory of the second contact point (100 V/100 V)

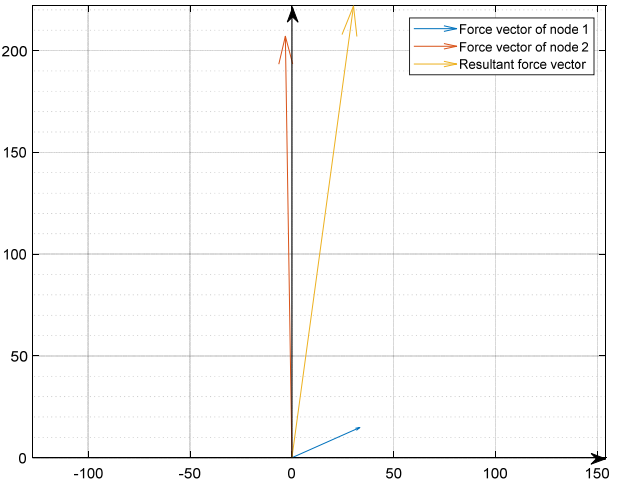

3c) $\varphi = 81.0527°$, $r = 216.1222$ nm

Fig. A32. Motion trajectories of contact points of a 11.5 mm × 13 mm × 9 mm hemisphere

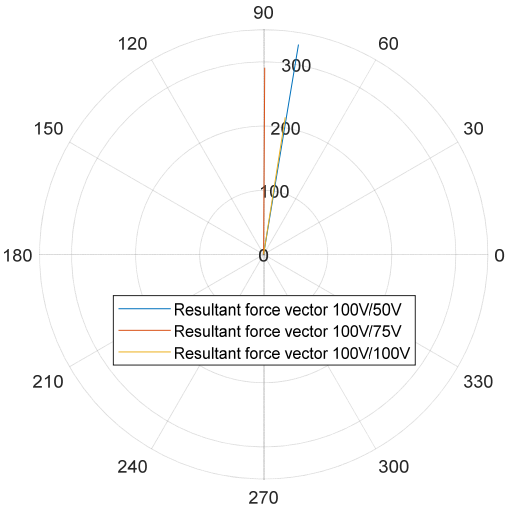

Fig. A32. Resultant force vectors in polar coordinates of contact points of a 11.5 mm × 13 mm × 9 mm hemisphere